ESTABLISHING A PATIENT DERIVED ORGANOTYPIC SLICE CULTURE MODEL OF GLIOBLASTOMA MULTIFORME

by

Liam Patrick Rappoldt

Submitted in partial fulfilment of the requirements
for the degree of Master of Science

at

Dalhousie University
Halifax, Nova Scotia
April 2021

TABLE OF CONTENTS

List of Tables

List of Figures

Abstract

Glioblastoma Multiforme (GBM) is the most common primary malignant brain tumour and has a median survival of 15 months. Despite many years of research in the field, prognosis remains dismal, due in part to the majority of the research being performed using monolayer cell culture, which does not represent the complexity of GBM. To partly address this gap in research models, I have generated and utilized a viable patient derived organotypic slice culture model. I have utilized this model to validate genetic manipulation via lentiviral transduction by successfully delivering a far-red fluorescent marker. I further explored the feasibility of utilizing this model to understand patient derived extracellular vesicles (EVs) for the future use as a GBM biomarker in liquid biopsy. The establishment of this model will hopefully lead to insights in to GBM biology and how EVs further its malignancy.

List of Abbreviations Used

ACRI	Atlantic Cancer Research Institute
ATRX	X-linked mental retardation syndrome
BBB	Blood brain barrier
CCM	Conditioned culture media
CD	Cluster of differentiation
CMDI	Cellular and Molecular Digital Imaging Facility
CNS	Central nervous system
CRISPR	Clustered regularly interspaced short palindromic repeats
DNA	Deoxyribonucleic acid
DMEM	Dulbecco's modified essential medium
ECM	Extracellular matrix
EDTA	Ethylenediaminetetraacetic acid
EGF	Epidermal growth factor
EGFR	Epidermal growth factor receptor
ENU	N-ethyl-nitrosurea
EV	Extracellular vesicles
FACS	Fluorescence assisted cell sorting
FGF	Fibroblast growth factor
FVD	Fixable viability dye
FWB	FACS wash buffer
GBM	Glioblastoma Multiforme
GEMM	Genetically engineered mouse model

GFAP	Glial fibrillary acid protein
GSC	Glioblastoma stem cell
GVHD	Graft versus host disease
HA	Hyaluronic acid
HEK	Human embryonic kidney
H&E	Hematoxylin and eosin
HEPES	N-2-hydroxyethylpiperazine-N-2-ethane sulfonic acid
HGCC	Human glioblastoma cell culture
HIF	Hypoxia inducible factor
HIV	Human immunodeficiency virus
HM	Humanized mouse
HPSC	Hematopoietic stem and precursor cells
IBA-1	Allograft inflammatory factor 1
IDH	Isocitrate dehydrogenase
IL	Interleukin
MDSC	Myeloid-derived suppressor cells
MGMT	O^6-methylguanine-DNA methyltransferase
MISEV	Minimal information for studies of extracellular vesicles
miRNA	Micro Ribonucleic acid
MRI	Magnetic resonance imaging
mRNA	Messenger ribonucleic acid
NADPH	Nicotinamide adenine dinucleotide phosphate
NF1	Neurofibromatosis protein

NOD-SCID	Nonobese diabetic/severe combined immunodeficiency
NSC	Neural stem cells
NSG	NOD-SCID GAMMA
PBS	Phosphate buffered saline
PFA	Paraformaldehyde
PTEN	Phosphate and tensin homolog
PD-L	Programmed death ligand
PDOX	Patient-derived orthotopic xenograph
PEI	Polyethylenimine
PSQ	Penicilin streptomycin glutamine
PTFE	Polytetrafluoroethylene
qRT-PCR	quantitative reverse transcriptase polymerase chain reaction
RB1	Retinoblastoma protein 1
RPM	Revolutions per minute
SNP	Single nucleotide polymorphisms
TAM	Tumour associated macrophage
TCGA	The Cancer Genome Atlas
TGF	Transforming growth factor
TME	Tumour microenvironment
TMZ	Temozolomide
TP53	Tumour protein 53
TU	Transducing unit
T_{regs}	Regulatory T cells

VEGF	Vascular endothelial growth factor
VEGF-R	Vascular endothelial growth factor receptor
WHO	World Health Organization

ACKNOWLEDGEMENTS

Although there are many, many people who have made this thesis possible, I would like to take the time to extend my appreciation to a few of them.

First and foremost, I would like to thank my supervisor Dr. Adrienne Weeks. Her mentorship, patience, and dedication to my success have been invaluable. Her unrelenting hard work, compassion, and commitment to helping her patients both in the hospital and in the lab is inspiring. Dr. Weeks' example has set the bar for the researcher and clinician I hope to become. I would also like to thank Dr. Kathleen Attwood, who taught me everything I know in the lab. Her patience and incalculable hours spent with me on my work made this thesis possible, and I am truly grateful for that. The diligence and attention to detail Dr. Attwood brings to her science I will try to emulate in all my future work. I would also like to thank previous lab member and old friend Inhwa Kim, who set the foundation for this project.

I would like to my co-supervisor, Dr. Craig McCormick and my advisory committee, Dr. Sultan Darvesh, and Dr. Jim Fawcett, for their support and guidance throughout this project. I would also like to thank Dr. Jeremy Roy and his team at the Atlantic Cancer Research Institute for their collaboration. I would also like to thank all members of the labs of Dr. Denys Khaperskyy, Dr. Jennifer Corcoran, and Dr. Craig McCormick, as well as the Division of Neurosurgery who welcome me into their division and who were fantastic collaborators in this project. A very special thank you to the patients who agreed to participate; their bravery and willingness to contribute made this study possible.

Lastly, I would like to thank my family, who have unwaveringly supported me in the pursuit of my dreams. This is as much their success as it is mine.

CHAPTER 1 INTRODUCTION

1.1 Glioblastoma Multiforme

Glioblastoma multiforme (GBM), the most malignant form of diffuse astrocytoma, is one of the deadliest forms of cancer (Stupp et al., 2005). GBM originates within the brain parenchyma and presents with symptoms related to invasion of surrounding brain, seizures or symptoms of increased intracranial pressure (DeAngelis, 2001). In general, diffuse astrocytomas are separated into grades two to four based on presence of cellular atypia, nuclear atypia, vascular proliferation and necrosis (Vigneswaran et al., 2015). The latter two being hallmarks of the highest grade (IV) diffuse astrocytoma termed GBM. GBM have the most aggressive pathology, histologically characterized by pseudo-palisading necrosis, microvascular proliferation and nuclear atypia, and consequently the worst prognosis (Louis, 2007; WHO, 2016). GBM carry an incidence rate of 3.19 per 100,000 individuals in the United States (Thakkar et al., 2014), with the median age of 64 years at diagnosis (Chakrabarti et al., 2005; Ostrom et al 2013; Tamimi and Juweid et al., 2017). GBM accounts for 54% of gliomas (Louis et al., 2016), making it the most common malignant brain tumour. Historically it was theorized that astrocytoma arose from differentiated, mature astrocytes (Sinai et al., 2005), however the more recent data has suggested that the astrocytoma cell of origin is tumour-initiating cell which has stem-like properties (Singh et al., 2003; Llaguno et al., 2009, 2019).

GBM typically occurs in the supratentorial brain parenchyma (Ohgaki et al., 2005). GBM is composed of a central necrotic core encompassed by actively proliferating cells that quickly invade to surrounding areas of the brain (WHO, 2017). Diagnosed microscopically based on cellular heterogeneity, microvascular proliferation, and necrosis, GBM is a highly aggressive malignancy, being classified as a grade IV astrocytoma (WHO, 2016) with very poor prognosis

(15 months (Stupp et al., 2005)) and limited effective treatments. GBM can either be classified as a primary GBM or a secondary GBM. Primary GBM arises *de novo* with no previously diagnosed lower grade lesion, typically in older patients (Vigneswaran et al., 2015). Secondary GBM arises from a lower-grade II diffuse astrocytoma, occurs in younger patients and has a slightly better prognosis (Huse et al., 2014). Although histologically identical primary and secondary GBM differ genetically which will be discussed below and is reviewed in **Table 1**.

Table 1. WHO Classification of diffuse gliomas. Adapted from Vigneswaran et al. (2015)

Tumour Type	WHO Grade	Histological Description	Median Survival (years)
Astrocytoma	II	Found diffusely infiltrating into surrounding neural tissue, increased hypercellularity, no mitosis	6-8
Oligodendroglioma	II	Occur in white matter and cortex of cerebral hemisphere, low mitotic activity, no necrosis	12
Anaplastic Astrocytoma/Oligodendroglioma	III	Highly infiltrative to surrounding neural tissue, increased mitotic activity, no necrosis or vascular proliferation	3
Glioblastoma	IV	Highly infiltrative, necrosis, highly mitotic, microvascular proliferation	1-2

The genomic revolution has allowed for extensive genetic profiling of GBM. The Cancer Genome Atlas (TCGA), with the goal of cataloging the genetic abnormalities in GBM cells, analyzed a more than 500-patient cohort to evaluate gene expression, single nucleotide polymorphisms (SNPs), and copy number variations to hopefully elucidate some of the genetic aberrations driving GBM. The gain of copies of chromosome 7, losses of chromosome 10, along with mutation in epidermal growth factor receptor (EGFR) are commonly identified in primary GBM (Waller et al., 2013; Sahm et al., 2014). Mutations in tumour protein 53 (TP53), Isocitrate dehydrogenase-1 (IDH-1), and ATRX are commonly found in secondary GBM (Waller et al.,

2013; Sahm et al., 2014). Other common mutations found in GBM are phosphate and tensin homolog (PTEN), platelet-derived growth factor receptor-alpha (PDGFR-a), neurofibromatosis type-1 (NF1), retinoblastoma protein (RB1) (Phillips, 2006). Verhaak et al. classified GBM as neural, proneural, classical and mesenchymal molecular subtypes based on clustering of expression of signature genes (Verhaak et al., 2010). However, each individual tumour is made up of every molecular subtype and this clustering has not yielded new therapeutic strategies (Qazi et al., 2019). Despite this extensive molecular subtyping novel treatment paradigms based on genomic analysis has not led to significant therapeutics unlike other malignancies such as breast cancer (Verret et al., 2020). In GBM, molecular profiling has not yet led to the same dramatic alterations in clinical treatment. Molecular criteria of these subtypes have the potential to direct therapeutics of GBM.

However, there are some genetic alterations common in GBM that can help predict treatment response. Most notably, IDH mutational status, O^6-methylguanine-DNA methyltransferase (MGMT)-promotor methylation status, and 1p19q codeletions (Yang et al., 2020) in GBM. IDH mutations have been shown to have favourable prognosis compared to wildtype IDH tumours. IDH mutations have become a defining feature of lower-grade diffuse astrocytomas and secondary GBM (Sanson et al., 2009). MGMT promotor methylation status is most relevant in the context of treatment response to TMZ, as it determines the tumour's ability to repair DNA damage exerted by TMZ (Hegi et al., 2005). Codeletion of 1p19q is a hallmark for diagnosis of the oligodendroglioma subtype of diffuse astrocytoma and carries with it a better prognosis and response to chemotherapy. (Weistler et al., 2014; Zhao et al., 2014). Finally, the ATRX gene was first discovered in X-linked mental retardation syndrome (ATRX syndrome) and functions in chromatin remodeling to maintain genomic stability (Pekmezki et al., 2017).

Although evidence does not suggest ATRX is a driver mutation gene, it can induce genomic instability that further results in mutation and progression of GBM (Koschmann et al., 2016). ATRX's role specifically in GBM is largely unknown however, there is a strong association in ATRX and IDH mutation, and low concurrence of 1p19q codeletion (Kannan et al., 2012). Therefore, ATRX mutation is predictive of lower grader astrocytoma, as opposed to 1p19q codeletion which predicts oligodendroglioma (Cai et al., 2015; Koschmann et al., 2016). In GBM specifically, ATRX expression is varied. Lowered ATRX expression is observed more in primary GBM than lower grades, indicating it may be a marker of malignancy (Cai et al., 2015).

Table 2. Review of glioma markers which aid in diagnosis and prognostication of glioma. Adapted from Vigneswaran et al. (2015).

Marker	Diagnosis	WHO Grade	Prognosis
IDH-1	Glioma, 2° GBM	WHO >II	PFS > 5 years
1p19q	Oligodendroglioma	WHO > II	Progression free survival >5 years
MGMT	No diagnostic role	WHO III-IV	Improved response to TMZ
+7/+10	1° GBM, progression	WHO III-IV	Poor
ATRX	Astrocytoma	WHO >II	Decrease in PFS

WHO, World Health Organization; PFS, progression free survival.

GBM has proved challenging to treat clinically and thus there has been limited progress in patient survival over the century since GBM was first classified (Cushing and Bailey, 1926; Bs et al., 2009; Stoyanov and Dzhenkov, 2018). The current treatment paradigm consists of maximal safe surgical resection followed by concomitant radiation and temozolomide chemotherapy (Stupp, 2005). GBM is a highly heterogenous, diffuse and invasive tumour, making complete resection impossible and thus treatment failure results typically in local recurrence and fatality (Louis et al., 2016). The greatest leap in survival in the modern era came with the addition of the MGMT alkylating agent temozolomide (TMZ) in combination with radiation, this led to an increase in median survival from 12 months to 15 months (Stupp et al., 2005). However, this survival is increased in those individuals with methylation of the MGMT

promoter, individuals with methylated MGMT have a median overall survival of 22 months, whereas individuals with unmethylated MGMT have a median overall survival of 15 months (Hegi et al., 2005).

1.1.1 GBM Tumor Microenvironment

The hallmark of GBM is necrosis, microvascular proliferation, and extensive heterogeneity (Noroxe et al., 2016) (Figure 1.1). Healthy tissue microenvironments in general are comprised of cooperating cells that provide support and can direct organ-specific function (Barcellos-Hoff et al., 2009). The brain consists of a highly specific parenchyma consisting of neurons, astrocytes, oligodendrocytes, and microglia, and is supplied by a unique vasculature separated from the rest of the periphery by the blood-brain barrier (BBB) (Barcellos-Hoff et al., 2005). However, GBM invades and hijack this carefully constructed 3-dimensional (3D) architecture, destroying its function, leading to advanced progression (Moran et al., 2005). These 3D tissue microenvironments, which initially provide anti-tumor interactions with the malignant cells (Barcellos-Hoff et al., 2001), are remodeled to formulate a niche where GBM cells thrive, and, in most cases (90%), recur in the same location following even the most aggressive treatment (Stupp et al., 2005). The extracellular matrix (ECM) of GBM serves as a scaffold on which the malignant cells grow and migrate (Toole et al., 2004). The main component of the brain ECM is hyaluronic acid (HA). HA is constitutively produced by GBM tumours and has been shown to associate with proliferation and infiltration through binding of its cellular receptor CD44, which is also overexpressed in GBM (Narayanan et al., 2012; Rape et al., 2014). The GBM ECM also responds provides cues in the TME, especially from the vasculature associated with the tumour. Molecules of collagen, laminin, and fibronectin

are present in relatively high abundance on the basolateral membrane of the GBM-associated vessels and have been shown to induce GBM cell proliferation, migration, and survival (Lathia et al., 2012). The proteoglycan tenascin-C has also been shown to be produced by GBM and its presence is correlated with angiogenesis and progression from low grade to high grade astrocytoma (Mahesparan et al., 2003). The binding of many of these ECM factors are controlled by membrane spanning proteins called integrins and the binding of integrin has been shown to negatively correlate with drug induced apoptosis in GBM (Aoudjit et al., 2001). Adhesion of integrins to their ligands of laminin, fibronectin and collagen desensitize GBM cells to therapy (Helgans et al., 2007). Tumour cells also release cell-secreted proteases, priming the tumour microenvironment (TME) for tumour growth by creating space and removing steric barriers, allowing for the uninhibited growth of the tumour and recruitment of necessary vasculature (Rape et al., 2014). For example, matrix metalloproteinases (MMPs) are a group of enzymes generally known to be responsible for the progression and degradation of ECM in oncogenesis and are upregulated in GBM patients, especially those with poorer prognoses (Kessenbrock et al., 2010).

The GBM TME is composed not only of tumour cells but normal parenchymal cells which contribute to more than 30% of the tumour mass (Charles et al., 2011) (**Figure 1)**. There is increasing evidence that the vasculature of GBM not only provides an exchange medium for nutrients and waste products, but also contributes structurally to GBM's perivascular niche (Rape et al., 2014). The perivascular niche in which GBM thrives consists of endothelial cells, pericytes and astrocytes (Chekenya et al., 2007; Charles et al., 2011). Furthermore, astrocytes found in the TME deploy autocrine signals to promote GBM survival, such as stromal cell-derived factor 1 (SDF-1), which is a developmental cytokine used by normal tissues to promote

healing of CNS lesions, but in cancer promotes tumor survival and progression (Barbero et al., 2002). Interestingly, this pro-tumour function of TME astrocytes appears to be an acquired phenotype. At the tumour's early stages, astrocytes tend toward protecting healthy cells from damage caused by the tumour (Nieland et al., 2020). As the tumour progresses, astrocytes lose their protective role and shift toward a pro-tumourogenic phenotype (Nagashima et al., 2002).

Figure 1. Glioblastoma Multiforme Tumour microenvironment. Adapted from Simon et al., 2020.

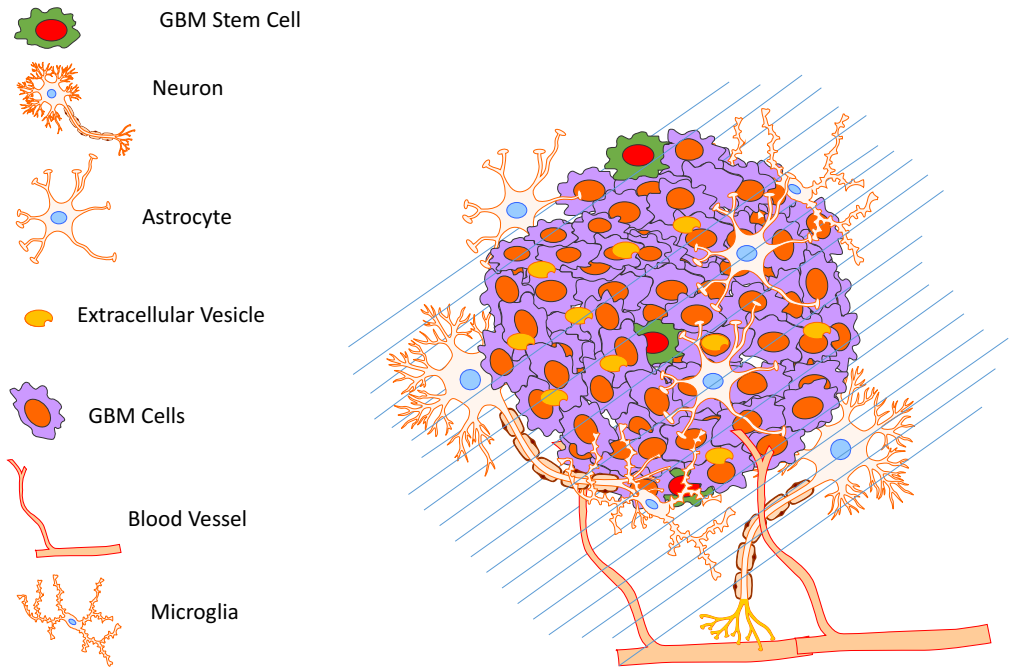

A hallmark of GBM is angiogenesis, with the recruited vasculature being crucial in tumour progression. However, it is irregular on two fronts: firstly, the basement membrane of brain capillaries becomes increasingly permeable, and secondly, angiogenic signaling stays active allowing the tumor to recruit new blood vessels (Haar et al., 2012; Wang et al., 2017). This facilitates exceptionally rapid growth; however, this rapid growth results in the tumour size rapidly outpacing new angiogenesis thereby creating a hypoxic environment and the pathogenic necrosis present in GBM (Ackerman and Simon, 2014). This hypoxic microenvironment is further propagated as the recruited vascular is leaky and is thus termed "neo-angiogenesis" (Gould and Cortneidge, 2014). Despite this highly hypoxic microenvironment, GBM tumours continue to thrive. GBM cell-induced angiogenesis is orchestrated by hypoxia-inducible factor 1 (HIF-1), a transcription factor cells use to detect low oxygen concentration (Shweiki et al., 1992; Maxwell et al., 1997), which induces aberrant VEGF signalling and the resulting neo-angiogenesis. This aberrant VEGF signalling and increased microvascular proliferation is key in GBM, and has gained interest as a potentially actionable target in GBM (Guarnaccia et al 2018). For example, bevacizumab is a monoclonal antibody against VEGF and has been used in the treatment for recurrent GBM, though its effects are only transient, and recurrence is not avoided (Li et al., 2017).

The brain vasculature is typically a fine balance of interactions between endothelial cells, pericytes and astrocytes, which together form the blood-brain barrier (BBB) (Jain et al., 2007). The (BBB) selectively restricts passage of movement between the periphery and CNS via tight junction regulation between endothelial cells, preventing large (>500 kadam) hydrophilic molecules from entering the brain (Jain et al., 2007). This restrictive nature contributes to drug resistance by GBMs by prohibiting many therapeutics from crossing over the BBB into the brain

parenchyma (Palmieri et al., 2007). When GBM grows to 1-2 cm in diameter, their infiltration compromises the BBB surrounding the tumour, both structurally and functionally (Fidler et al., 2002). This size represents a critical mass that warrants the recruitment of new blood vessels (Kim and Lee, 2009) to compensate for both the rapid growth of the tumour and the disruption of the regular blood supply that has been compromised by BBB disruption (Carmeliet, 2003). This recruitment occurs by angiogenesis; the microvascular proliferation of endothelial cells to form new blood vessels from pre-existing vasculature (Carmeliet, 2003). Angiogenesis is typically a well-controlled balance of pro- and anti-angiogenic factors (Folkman et al., 1971; Folkman et al., 1991; Fukumura et al., 1998) secreted by endothelial cells, stromal cells, and blood cells (Dameron et al., 1994). However, GBM cells can disrupt this balance by secreting an increased amount of proangiogenic signaling molecules, such as vascular endothelial growth factor (VEGF), basic fibroblast growth factor (bFGF), among others (Good et al., 1990). Additionally, enzymes such as serine proteases and matrix metalloproteases (MMPs) degrade the ECM, further propagating the aberrant angiogenic signaling (Fang et al., 2000).

As GBM is such a rapidly growing tumour, it quickly outgrows its vasculature, resulting in deficits in blood supply. This hypoxic state is believed to trigger angiogenesis (Kim and Lee, 2009) by activating hypoxia-inducible factor 1 (HIF-1), a transcription factor cells use to detect low oxygen concentration (Shweiki et al., 1992; Maxwell et al., 1997). HIF-1 regulates expression of many angiogenesis- and glucose metabolism-related genes, and activates the appropriate signaling molecules to initiate angiogenesis, most importantly, VEGF. Accordingly, there is high VEGF mRNA expression levels in hypoxic regions of GBMs, and VEGF receptors (VEGFR1 and VEGFR2) have been found to be highly expressed in astrocytomas as well (Plate et al., 1992; Samoto et al., 1995). Moreover, mRNA expression profiles in patient GBMs have

shown expression of proangiogenic factors (Tso et al., 2006). Crucially, the resulting microvascular proliferation is partly diagnostic criteria of GBM (Yano et al., 2000). The GBM vascular anatomical structure formed by tumour-associated vessels also provides a pro-survival environment, known as the perivascular niche (Rape et al., 2014). As previously mentioned, it is composed of pericytes, astrocytes, and endothelial cells, and is essential for pro-tumour survival through autocrine signaling, primarily from astrocytes (Charles et al., 2012; Rape et al., 2014).

The excessive VEGF signaling causing this hyper-proliferation and recruitment of endothelial cells is detrimental to the integrity of the tumour's blood supply (Monteiro et al., 2017). Pericytes that normally provide coverage and support to the sprouting blood vessels are relatively underdeveloped, resulting in defective and permeable blood vessels that easily and frequently collapse, leading to hypoxic foci and the necrotic core within GBM (Yuan et al., 1994; Wrinkler et al., 2004; Carmeliet et al., 2011). Hypoxia is a fundamental characteristic of GBM and is thought to be a major problem in the treatment of GBM as it promotes tumour cell invasion into surrounding healthy tissue (Kaur et al., 2005; Yang et al., 2012). Although fundamental to its pathogenesis, hypoxia is not unique to GBM as it is common in many solid tumours which experience an expansion and therefore increased oxygen diffusion distance (Carmeliet et al., 2011). This occurs when the oxygen demand of the cell exceeds oxygen supply available to the cell, resulting in the overall deprivation of the cell of necessary oxygen levels and can be visualized in GBM by tumour vascularity on contrast enhanced MRI (Clara et al., 2014; Jensen et al., 2014). This contrasts with normoxia, known as a condition of sufficient oxygen supply for the cell to conduct necessary processes in which normal parenchyma live (Kulkarni et al., 2007).

GBM cells survive in this harsh, hypoxic environment that normally causes cells to halt proliferation and eventually undergo apoptosis (Grieger and van der Wall, 2004; Shibao et al., 2018). There is strong evidence that the ability of GBM to resist treatment is due significantly to this capacity to survive in the necrotic, hypoxic core of the tumour (Haar et al., 2012). For instance, this ability to endure the hypoxic core of the tumour allows the cells to persist in a somewhat sheltered environment, where the vasculature is not present and therefore chemotherapeutic treatment is unable to reach its target (Vaupel et al., 2001). Another factor is that cells present in hypoxic areas of the tumour are not proliferative, and therefore are intrinsically immune to the anti-proliferative actions of many anticancer agents (Oliver et al., 2009).

The immune system plays an active role in GBM. As the development of GBM is a multi-step process that accumulates genetic and epigenetic changes that drive tumour progression, these changes distinguish GBM from normal cells and allow GBM to be recognized as foreign by the immune system (Mellman et al., 2011; Gros et al., 2014). However, tumours seldom get rejected by the immune system spontaneously, reflecting the ability to foster an immunosuppressive TME (Chen et al., 2013). The GBM TME includes high counts of macrophage/microglia and low counts of T cells (Chen et al., 2013). Although the levels of T cells are low in GBM TME, T cell infiltration positively correlates with outcome (Chen et al., 2013). Although in principle tumour associated macrophages and microglia (TAMS) can attack GBM cells presenting foreign antigens and present those antigens to T cells to generate an immune response, TAMS typically contribute to immunosuppression as evidenced by their heightened levels being associated with poorer prognosis (Poon et al., 2017; Broekman et al., 2018). GBM produce immunosuppressive molecules such as TGF-B and interleukin (IL)-10 and

can express immune checkpoint ligands that markedly inhibit immune cell effects such as programmed dead ligand 1 (PD-L1) (Garber et al., 2016; Hodges et al., 2017). Immunosuppressive molecules such a TGF-B and IL-10 recruit immunosuppressive cells such as regulatory T cells (T_{regs}), myeloid-derived suppressor cells (MDSCs) and TAMS. Notably, recruitment of TAMs, MDSCs, and T_{regs} has been correlated with poor overall survival (Yue et al., 2014). Research has attempted to reinvigorate immunity against GBM, with promising antitumour immune responses in preclinical studies (Yan et al., 2015; Reardon et al., 2016; Hu et al., 2016; Kim et al., 2017; Speranza et al., 2018). These trials focus on immune checkpoint blockade, and although this modality has shown promising results preclinically, therapeutic benefit during clinical trials in GBM patients has been limited (Hu et al., 2021). Although challenging, harnessing the immune system to target GBM and modulate its immunosuppressive effects has promise as a GBM therapy (Hu et al., 2021).

1.2 Experimental Models Of GBM

Many obstacles hamper development of effective therapies, including pervasive tumour cell invasion, genetic heterogeneity, therapeutic resistance, BBB permeability, and inter-tumoural variation (Marques-Torrejon et al., 2018). Throughout GBM pathology, tumour cells disseminate widely across many regions of the brain, spanning over multiple microenvironments that consist of distinct repertoires of cell matrix, growth factors, and neighboring cell types (Marques-Torrejon et al., 2018). GBM stem cells (GSCs) have been shown to drive tumour growth and can form new, distinct tumours (Singh et al., 2004). These cells react to different environmental niches through which the GBM invades, creating an extreme heterogeneity depending on the location in the brain and the molecular signals to which it is subjected

(Piccirollo et al., 2015). Historically, GBM and most cancers have been studied in bulk by cellular monoculture, either with immortalized or primary cell lines. While these models have their advantages, they are devoid of many of the characteristics fundamental to GBM biology, such as heterogeneity, recruited vasculature, immune cells and the TME. A discussion of the various models of GBM is presented below.

1.2.1 Immortalized Cellular Culture

Classically, GBM has been studied mostly by using *in-vitro* immortalized monolayer cell culture. Cancer cells can be immortalized and be established when a cell loses its cell cycle checkpoint pathways, which can be done during experimental immortalization protocols that focus on overriding natural cellular senescence (Shay et al., 1991; Maqsood et al., 2013). These cell lines have facilitated cancer research in many ways and have shed light on functional aspects of tumour transformation, gene expression, drug screening, and mechanism of treatment resistance (Torsvik et al., 2014). Cancer cell lines represent important tools to study the genetic aberrations and molecular pathways of cancer. Cell lines are inexpensive, easy to manipulate, can be cultured for many passages, and are easy to expand (Kaur et al., 2012). However, a direct consequence of their extensive use is genetic drift, resulting in altered phenotypes from the original tumour (Torsvik et al., 2014). Studies have even shown that up to 30% of cell lines in use are misidentified (Lorsch et al., 2014; Ben-David et al., 2018)

For GBM research, a commonly used cell line is U251, which was derived from a male patient with a malignant astrocytoma (Ponten and Westmark, 1973; Torsvik et al., 2014). The U251 cell line serves as a reliable method to study GBM (Humpel, 2015). Unfortunately, cell line monolayer cultures have their drawbacks. These monocultures of genetically identical GBM-derived cell lines do little to recapitulate the actual biology of a disease as heterogenous

and genetically chaotic as GBM. This genetic homogeneity requires the use of other cell lines to validate results generated by U251s, as the data may not apply to genetically dissimilar cells. Given their long life in culture and selective pressures, immortalized cell lines such as U251s have experienced significant genetic drift resulting in a lack of genetic comparability to GBM or the original passages of the line (Torsvik et al., 2014). For example, long-term cultured clones have accumulated several additional genetic aberrations when compared with the original U251 cells, such as losing their GBM signature in the form of differential amplification of chromosomes 3, 7, 15, and 17 (Torsvik et al., 2014). Moreover, they also exhibit phenotypic changes of altered morphology, variable cell surface markers expression, increased growth rate and more aggressive cell growth *in vitro* (Torsvik et al., 2014). Specifically, particular long-term passage clones of GBM can differ in cytoskeletal arrangements and growth patterns compared to low passage U251 cells (Torsvik et al., 2014). Furthermore, due to their lack of extracellular matrix, supporting stroma, and overall heterogeneity (all crucial to GBM biology), immortalized *in vitro* monocultures fall short in clinical translation (Camphausen et al., 2005).

1.2.2 Primary Cellular Culture

An alternative to immortalized cell lines are patient-derived primary cells maintained in serum-free media. These cell cultures are generated directly from patient tumour tissues, and unlike immortalized cells they have not been genetically engineered to avoid normal senescence pathways (Alves et al., 2011). These are cultured for a limited number of passages in the presence of defined growth factors but in the absence of serum to prevent differentiation (Singh et al., 2003). With a shorter culture lifespan and the absence of iatrogenic genetic alteration, cultures retain much greater similarity to the primary tumour from which they were taken, and therefore their use enables the discovery of fundamental characteristics of GBM genetics.

Primary cellular culture has allowed for the discovery of stem-like cells, referred to as glioblastoma stem cells (GSCs) (Lee et al., 2006). Specifically, these cultures have been used to show that the GSC phenotype of GBM cells is induced and maintained in specific niches, including the hypoxic niche (Hiddleston et al., 2009; Li et al., 2009; Seidel et al., 2009; Seidel et al., 2010). It was also shown using these primary cells that GSCs possess enhanced radio- and chemo-therapeutic resistance, a phenotype that likely drives GBM tumour recurrence (Bao et a., 2006; Eramo et al., 2006). Use of primary cells has also shown that GSCs have a more potent ability to repopulate not only the tumour bulk but also stimulate formation of tumour vasculature cells such as endothelial cells and pericytes (Wang et al., 2010; Soda et al., 2011; Cheng et al., 2013). Primary GBM cells also have been employed to elucidate the role of inflammatory responses on tumour growth, as well as the interaction between GBM cells and immune cells. These findings show the recruitment of immunosuppressive macrophages by GSCs (Wu et al., 2010; Tafami et al., 2011; Yi et al., 2011). Although the applications of primary GBM cellular culture appears to surpass those of immortalized cellular culture, they still have drawbacks. One of the chief limitations is the fact that they are still grown in a tissue culture mono layer and as such lack all the microenvironmental characteristics important to GBM pathology (Rape et al., 2014). Furthermore, they are challenging to expand as their culture lifespan is limited due to their natural progression towards senescence (Hayflick and Moorehead, 1961; Hayflick, 1965).

To partly address the 2-dimensional (2D) limitation of cellular culture, primary GBM cell spheroid cultures grown in suspension have been implemented (Hemmati et al., 2003; Singh et al., 2003; Galli et al., 2004). These are genetically and transcriptionally relevant to the parent tumour, and the GSCs that emerge from the culture of these lines faithfully recapitulate GBM when transplanted *in-vivo* (deCarvalho et al., 2018). Moreover, they retain genetic disruptions

that were present in the parent tumour both when studied *in-vitro* long-term, as well as in resulting xenografts. Employing spheroid cultures further, they have been grown in Matrigel to create organoid cultures (Lancaster et al., 2013; Huch et al., 2017; Tuveson and Clevers, 2019). This ECM-like solution cultivated by Engelbreth-Holm-Swarm (EHS) mouse sarcoma cells has been exploited in the scientific community as a culture substrate to provide an environment like what would be found *in-vivo* (Hughes et al., 2010). The Matrigel scaffolding allows these organoid cultures to be grown to an increased size, thus exhibit many factors typical in an *in-situ* GBM, such as necrotic and hypoxic states, as well as the mosaic of proliferative, quiescent, and differentiated cell states present in GBM (Hubert et al., 2016). However, cerebral organoids are variable and are time-intensive to culture (Benton et al., 2009), thus presenting financial and temporal restraints on their usage for modeling GBM.

1.2.3 Animal Models

Whole animal models are the gold standard in cancer research, and GBM is no exception (Zhang et al., 2011). Mice are most commonly used as they are the most experimentally accessible option, offering ease of genetic manipulation, relatively short breeding time, and shared organ system and physiology to humans (Robertson et al., 2019). However, the C6 rat glioma cell line is less but still commonly used to model GBM in vitro and in vivo (Giakoumettis et al., 2018). Mouse models of GBM are established either by transplantation of tumour-initiating cells into mice, or autochthonous models where tumours are formed *de novo* by targeting genetic strategies, as summarized in **Table 3**. Transplanted mouse models can be allografts, where the implanted cancer cells are from same species, or xenografts, where the implanted cells are from a different species (Liu et al., 2015). Allografts and xenografts can be

either orthotopic (transplanted intracranially) or heterotopic (typically transplanted subcutaneously) (Ostom et al., 2013).

Orthotopic grafts are a more attractive route, as they provide the most accurate tissue context (Taillandier et al., 2003; Fei et al., 2010). Moreover, the manageable control of spatial and temporal initiation makes generating large cohorts of standard lesion-bearing mice experimentally achievable. However, the grafting procedure inherently produces an injury and disruption in the tissue architecture, and there is limited ability to control progression of the lesion once injected. Allografts of tumour cells generated from carcinogen-induced rodent astrocytoma or from transgenic mice have allowed for the modelling of immune studies *in-vivo* (Mahesparan et al., 2003; Kijima et al., 2014) as they do not produce any graft-versus-host disease (GVHD) in the mouse. More recently utilizing the advent of CRISPR technology, researchers have been able to generate tumourigenic neural stem cells (NSCs) that can be transplanted into isogenic mice with fully functioning immune systems (Qzi et al 2014). However, studies have shown that GBM cell line tumours generated in mice to not match patient GBM in the sense that they are lacking microvascular proliferation, tumour necrosis, and single-cell migration (Anderson et al., 2002; Mahesparan et al., 2003; Martens et al., 2008; Kijima et al., 2014).

When transplanting human cell lines or patient-derived cell lines, an immunocompromised or humanized mouse (HM) model is required to prevent graft rejection (Robertson et al., 2019). Humanized mice have been engineered to express human proteins considered relevant to tumour growth (Frese and Tuveson et al., 2016). This can be accomplished multiple ways, including genetic engineering, injection of human peripheral blood, implantation of human stromal tissue together with human tumour, and engrafting human hematopoietic stem and precursor cells

(HSPC) into sub-lethally irradiated immunocompromised mice (Shultz et al., 2005; Frese and Tuveson et al., 2007; Bankert et al., 2011). Transplanting into immunocompromised mice typically occurs into non-obese diabetic severe combined immunodeficient gamma (NOD-SCID-gamma, NSG) mice (Shultz et al., 2005). NSG mice have been engineered and bread to lack mature T- and B-cells, along with natural killer cells, and are among the most immunodeficient mouse models to date (Shultz et al., 2005 and 2020; Walsh et al., 2018). Immunocompromised or HM models are used to implant freshly isolated tumour cells without intervening culture steps to establish patient-derived orthotopic xenografts (PDOX), which have provided the best attempt at capturing relevant features while mostly sidestepping *in-vitro* selection (Jin et al., 2010; Hidalgo et al 2014). Crucial factors represented by PDOX are aspects of the TME, including vasculature, ECM, and some immune factors (Sakariassen et al., 2006; Wang et al., 2009; Fei et al., 2010; Jeswani et al., 2013; Robertson et al., 2019). However, PDOX models are costly and labour intensive to upkeep, and do not completely side avoid selection while the lesions are propagated through mice (Bed-David et al., 2017). This results in selection of particular subpopulations of tumour cells, and for the loss of TME as the mouse microenvironment takes over.

Genetically engineered mouse models (GEMMs) historically were generated by using chemical mutagenesis, inducing GBM formation in mice using N-ethyl-nitrosurea (ENU), which was first described by Schiffer and colleagues (1978). ENU-induced tumours in mice are valuable models of GBM because they harbour mutations commonly found in GBM, exhibit similar genetic heterogeneity to GBM, and arise in a TME relevant to GBM (Charles et al., 2010). However, the reproducibility of tumour formation is low in ENU-induced tumours and has therefore been phased out of use, especially with the advent of the genomic revolution and the ability to introduce defined genetic alterations (Robertson et al., 2019). Such autochthonous

models can carry germline mutations and bread selectively, giving rise to compound mutants with aberrations in oncogenes and tumour suppressor genes, allowing for the study of early initiating events in GBM and dictate how the tumour progresses (Alcantara Llaguno et al., 2019). The mutations are introduced using viral delivery systems and, since target genes are sometimes early lethal, are used in conjunction with conditional expression tools such as the widely used Cre-*loxP* recombinase system (Noorani et al., 2019). Conditional expression allows for induction of genetic manipulations at selected times, or in specific cell types (Alcantara Llaguno et al., 2015). An important mouse model for the study of primary GBM has been the NG2-CreER mouse, which combines TP53 loss and conditional loss of Nf1 (Zhu et al., 2005). Other useful and notable GEMMS have been summarized by Miyai et al. (2017) and include PTEN knockout mice (Wei et al., 2006), TP53 knockout mice (Marumoto et al., 2009), NF1/TP53 double knockout mice (Ding et al., 2001)., and IDH^{R132H} knock-in mice (Bardella et al., 2016).

Mouse models have become the most desired tool for studying tumour initiation, maintenance, progression, and response to treatment. However, mouse models present drawbacks. Specifically, in autochthonous mouse models, whether it be by breeding strategies or mice genetically engineered to spontaneously produce lesions, polyclonal tumour formation can complicate data, especially data surrounding mouse survival (Chen et al., 2012). As well, mouse models are laborious and expensive to generate, propagate, and maintain, thus leading to their use being limited to larger centers and labs (Cheon and Orsulic, 2011). Organotypic culture models may serve as a solution to this, as a compromise between cellular monoculture and expensive, time-intensive animal models.

Table 3. Summary of glioblastoma mouse models. Adapted from Kijima and Kanemura., 2017.

Model	Advantages	Disadvantages
Cell-line xenografts	High engraftment and growth rates Good reproducibility Reliable disease growth and progression	Does not recapitulate genetic and phenotypic feature of original tumour Need to use immunodeficient mice
Patient-derived xenografts	Recapitulate genetic and phenotypic features of original tumour	Relatively low engraftment and growth rates Need to use immunodeficient mice
Genetically engineered mouse models (GEMMs)	Identifies molecular events responsible for tumour initiation and progression Analyze the role of TME	Does not completely reflect the intratumoural genomic and phenotypic heterogeneity Tumour initiation cannot be controlled
Syngeneic mouse models	Suitable for tumour immunity and immunotherapeutic research	Might be different from human glioblastoma

1.2.4 Organotypic Slice Culture

Organotypic culture models may serve as a solution to this, as a compromise between cellular monoculture and expensive, time-intensive animal models. Both immortalized and primary cell lines do not represent the GBM TME, which has been shown to play a fundamental role in tumour biology (Humpel et al., 2015; Gould and Courtneidge, 2014; Simon et al., 2020). The TME is not just a supportive structure but plays a key role in a GBM tumour's ability to propagate through the brain, contributing to its invasive and aggressive nature (Aleves et al., 2011; Gould and Courtneidge, 2014). This complexity of the TME of GBM paints a vivid picture that the models of studying GBM and its pathobiology must recapitulate this diversity. Although much research still needs to be conducted on the GBM TME, it is worth considering that the stall in long-term treatment for GBM can be partly addressed by the model system used to study it.

Organotypic models are so named as they are typical of the origin in which they are harvested from (Humpel, 2015). They were first established in the mid 20th century using chick embryo eyes (Gawhiler et al., 1981). Although development of CNS organotypic models began in the 1960's, the first successful attempt of the CNS occurred in 1981 by Gawhiler et al, using the roller-tube method. This method involved thinning the CNS tissue into a plasma clot or collagen matrix on coverslips in a sealed tube that could rotate in a roller incubator (Humpel, 2015). This was eventually improved in 1991 by Stoppini et al., resulting in the currently used membrane-interface method of semipermeable membranes. This allowed for the slices to obtain nutrients by capillary action through the membrane, without sacrificing gas exchange at the top of the slice (Dionne and Tyler, 2013). This method filled a gap between *in vitro* and *in vivo* cell culture and has become widely used as a result (Dionne and Tyler, 2013).

Organotypic models are advantageous for three important reasons. Firstly, the stromal context is preserved which is crucial when culturing GBM, as tumour cells are spread across a multitude of brain regions, spanning multiple TMEs (Marques-Torrejon et al., 2018). Secondly, the semipermeable membrane in which it sits allows researchers to manipulate the experimental conditions and observe the GBM slice's response. Lastly, supernatants can be collected for analysis to analyze a wide variety of factors such as signaling molecules and extracellular vesicles (see section 1.3) (Merz et al., 2013). Although promising, there are limitations to organotypic modelling of GBM. The removal and slicing of tissue inevitably damages axons, causing the slice to lose its innervation ultimately resulting in cell death (Humpel, 2015). Moreover, they are more susceptible to contamination throughout the harvesting process. The genetic variability between patient-derived slices introduces challenges in experimental reproducibility, although this can be overcome by increasing experimental replicates. However,

using a model from many patients may increase the generalizability of therapeutic data derived from this model. It is also worth mentioning that the lack of normal vasculature in the slices does not fully recapitulate the nutrient delivery found *in vivo,* as the slices are nourished by diffusion of oxygen from the culture environment (Humpel, 2015). Furthermore, organotypic slice culture addresses a gap in the current modelling of GBM, hopefully branching between intracellular signaling mechanisms and tissue level biology (Shamir and Ewald, 2014).

The use of organotypic cultures in GBM research has been steadily increasing. Parker et al. (2017) used a human GBM organotypic culture model to study tumour invasiveness and migration. Previously to this, Merz et al. (2013) utilized organotypic models to successfully show different susceptibilities to treatments according to the methylation of MGMT in GBM patients. Groups using organotypic models of GBM have investigated heavy ion irradiation which has allowed this research to precipitate into clinical trial (Merz et al., 2013). Further, Merz et al. (2013) also reinforced MGMT's role in susceptibility of the GBM slice to treatments, showing the relationship between methylation status of its promotor and ability to carry out that branch of DNA repair.

Organotypic slice culture is to investigate the roles of GBM-associated genes and their roles in the tumour's biology. Parker et al. (2017) used general gamma-retrovirus to infect GBM organotypic culture to study migration and invasion. Lentiviruses are another type of retrovirus that introduce exciting possibilities for study of GBM. Lentiviruses are enveloped particles containing homodimers of the linear single-stranded RNA genome (Denning et al., 2013). These viruses stably integrate into the genome of host cells they infect, allowing stable expression of a gene of interest (Wollebo et al., 2013). Derived from human immunodeficiency virus (HIV)-backbone lentiviruses contain a modified vesicular stomatitis virus G (VSV-G) envelope giving

them an increased range of lentiviral host cells (Wallebo et al., 2012). Their ability to infect both dividing and non-dividing cells and versatile VSVG envelope has made them an extensively used vector for fundamental biological research (van Hooijdonk et al., 2009). Lentiviral vectors can be used in second generation systems that are divided into packing plasmid, envelope plasmid, and the plasmid that holds the gene of interest (Zuffrey et al., 1999). Genetically engineered to only be able to replicate once within a carrier cell line (Dull et al., 1998) they are a relatively safe way to insert genetic information directly into the cells of interest, and therefore have become a widely used tool in the study of cancer. Retroviruses can be used to transduce fluorescent genes (Parker et al., 2017) into cells or sequences that code for clustered regularly interspaced short palindromic repeats (CRISPR)-Cas9 systems that can be used for genome editing (Cong et al., 2013). Attwood et al. (2020) used this CRISPR-Cas9 lentiviral system to interrogate genes associated with integrated stress response, and how genetic disruption of these genes affected GBM cells' ability to cope with hypoxia, a fundamental feature of GBM. Considering this, lentiviral vectors have been used and validated as an efficient and powerful tool for transgene delivery (Kutner et al., 2009).

1.3 Extracellular Vesicles

Extracellular vesicles (EVs) are lipid-bilayer bound particles that are released from many mammalian cells (Margolis and Sadovsky, 2019). EVs carry a cargo of proteins, nucleic acids, lipids, and metabolites from the parent cell, and have a wide variety of biological functions ranging from cellular waste disposal to paracrine signaling (Yanez-Mo et al., 2015; Andre-Gregoire et al., 2017, Thery et al., 2018). The transfer of EVs from cell to cell in a paracrine fashion, in both healthy and malignant tissue, has allowed them to gain attention in cancer biology in recent years. In GBM, EVs have shown to have many tumour promoting effects

including angiogenesis, invasion, resistance to drugs and evasion of apoptosis (Mondal et al., 2017; Simon et al., 2018). Moreover, analysis of EV content has shown to reflect that of the parent cell (Lane et al., 2019). This, along with their ability to be detected in the bloodstream, make EVs a potential non-invasive biomarker, specifically in the context of liquid biopsy (Loo et al., 2019; Osti et al., 219) In a quickly growing field, much of the work has been conducted using bulk analysis of vesicles using protein or RNA components (Shao et al., 2012; Im et al., 2014). However, there has been a lack of ability for these studies to accurately characterize individual vesicle anatomy. Single EV analysis has recently become an exciting frontier to provide insight into tumour-derived EVs and their function (Fraser et al., 2018).

In the GBM microenvironment, evidence is such that EVs contribute to tumour progression by recruiting essential vasculature, suppressing the immune system, and aiding in communication with surrounding tumour cells, and therefore have gained intense interest in the last few years due to their role in other cancers (D'Asti et al., 2016; Pucci et al., 2016; Tkach and Thery, 2016). GBM, with its fast growth and resulting hypoxic regions, relies heavily on neo-angiogenesis (Simon et al., 2017). For this to occur, endothelial cells must proliferate, and form organized tubular structures, a process termed neo-angiogenesis, that EVs mediate by VEGF signaling (Nareshkumar et al., 2018; Virtanen et al., 2021). Interestingly, Sun et al. (2017) found that GBM cells *in vitro* transfected with a miR-21, promoted endothelial cells to form tubular structures and Wang et al. (2019) were able to identify miR-26 in recipient GBM cells *in vitro*. Tubular structure formation in vitro is a powerful tool to detect for the in vitro screen of a factor's ability to promote angiogenesis in vivo (Fukushima et al., 2008; Mukai et al., 2008; Arnoutova et al., 2009: Arnaoutova et al., 2010). This indicates that not only are GBM EVs responsible for vascular recruitment in the TME, but specific miRNAs within them are able to

spur angiogenesis in non-cancerous cells within the TME (Mondal et al., 2017; Sun et al., 2017; Wang et al., 2019). Additionally, Oushy et al. (2018) showed that miRNA crosstalk between another component of the TME vasculature, astrocytes, further propagates GBM cell growth *in vitro*.

EVs also contribute to immunosuppression in the GBM TME, and have been shown to assist in GBM immune evasion through the programmed death receptor 1 (PD-R1). This is not exclusive to GBM, as PD-R1 related agonism is also of benefit to melanoma by fostering tumour-promoting humoral immunity in the lymph node (Yanez-Mo et al., 2015; Pucci et al., 2016; Ricklefs et al., 2018). EVs are capable of changing the landscape of recruited immune cells to the tumour by promoting an immunosuppressive M2 microglia phenotype through microRNAs (miR-451 and miR-21) and interleukins, (IL-6, TGF-Beta, etc.) (Guo et al., 2019). This immunosuppressive pro-tumour effect is elicited in other cell types as well, including myeloid-derived suppressor cells (MDSCs) and T cells, and contributes to the shift from an anti-tumour microenvironment to a pro-tumour microenvironment (Baulch et al., 2016; Ricklefs et al., 2018; Brown et al., 2018; Grimaldi et al., 2019).

These EVs have been found to be highly heterogenous in GBM patient serum (Fraser et al., 2018), with interesting aberrations in gene expression compared to healthy control samples (Noerholm et al., 2012). Skog et al. (2008) showed that there is a population of EVS in GBM patient plasma that had a matching EGFRvIII signature to the tumour tissue. Osti et al. (2019) also found a significant EV enrichment in the plasma of GBM patients compared with plasma of healthy patients. To elucidate what EVs are doing, Skog et al. (2008) further investigated EVs in culture. They found EVs isolated from patient plasma are able to stimulate tubule formation by endothelial cells and proliferation of an astrocytoma cell line (Skog et al., 2008).

Figure 2. Extracellular Vesicles. (A) Composition of extracellular vesicles. **(B)** Stimulation of neo-angiogenesis by GBM-derived EVs as example of pro-tumour effect of EVs. Adapted from Ricklefs et al. (2016) and Simon et al. (2020).

A

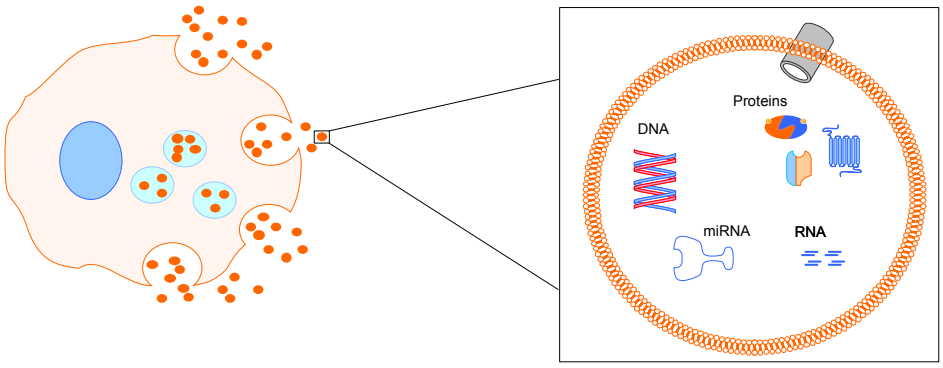
Proteins
DNA
miRNA
RNA

B

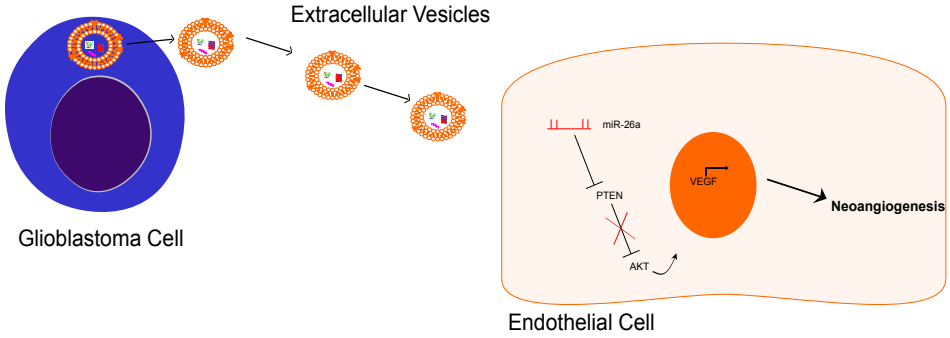
Extracellular Vesicles
Glioblastoma Cell
miR-26a
PTEN
AKT
VEGF
Neoangiogenesis
Endothelial Cell

This, along with work showing EVs' ability to induce tumor progression and infiltration, has rationalized interrogation of their role in GBM. The isolation of the EVs from the proposed organotypic slice culture model could further the utility of the model to study EVs. Specifically, analysis of EVs isolated from the tumour samples, along with matched EVs from the patient serum, has attractive application for potential liquid biomarkers, both to track progression and reveal diagnosis of GBM prior to imaging or invasive craniotomy.

1.4 Overview

GBM is a uniformly fatal malignancy without an effective cure. GBM is an extremely aggressive, invasive and resistant tumour that carries a median survival of approximately 15 months with maximal safe intervention. The field of GBM research is needing a new way to translate improved understanding of the tumour biology into meaningful treatment options and a recapitulative method of studying GBM pathobiology.

In this thesis I have presented the development of an organotypic slice culture model of patient-derived GBM samples that will allow for a representative model of GBM to fit in the niche between *in-vitro* cell culture and *in-vivo* animal models. Following the establishment of this culture model, I have demonstrated its ability to be genetically manipulated using a far-red fluorescent lentiviral vector. We have utilized the organotypic slice culture model to identify EVs in the conditioned media from the slices. As GBM EVs have been identified in patient serum (Fraser et al., 2018), we hope to isolate the same EVs signature from the GBM slice media to give a robust tool to study GBM EVs. Together, this model hopes to yield a better way of GBM culture that will further our understanding of this devastating malignancy.

CHAPTER 2 MATERIALS AND METHODS

2.1 Cell Culture

U251 immortalized human glioblastoma cells (cat # 09063001, European Collection of Authenticated Cell Culture) and Human Embryonic Kidney (HEK) 293T cells (cat # CRL-1573) were acquired from Millipore Sigma and ATCC, respectively, and were cultured in Dulbecco's Modified Essential Medium (DMEM) supplemented with 10% heat inactivated fetal bovine serum (HI-FBS) and 100 U/mL penicillin, 100 µg/mL streptomycin, 2 mM L-Glutamine (PSQ) (Thermo Fisher Scientific). U3024 (RRID: CVCL_IR67) and U3085 (RRID: CVCL_IR95) primary glioblastoma cell lines were acquired from Human Glioblastoma Cell Culture (HGCC) and were cultured on 10 µg/mL poly-L-ornithine (Sigma Aldrich) and 10 µg/mL laminin (Sigma Aldrich) coated plates in 1:1 Neurobasal and DMEM/F12 Glutamax supplemented with 100 U/mL penicillin, 100 µg /mL streptomycin, 1X B-27 supplement , 1X N-2 supplement (Thermo Fisher), 10 ng/mL epidermal growth factor (EGF) and 10 ng/mL fibroblast growth factor (FGF) (Peprotech). All cell lines were cultured at 37 °C with 5% CO_2.

2.2 Organotypic Slice Culture

Intra-operative GBM samples were acquired following patient consent (REB # 1023343) and transported to the lab in phosphate-buffered saline (PBS, Thermo Fisher Scientific) on ice. Tumour tissue was sliced using the Vibratome 3000 Sectioning System generously provided by the Zhang lab. The tumour tissue was glued onto a 3% ultrapure agarose block mold and was subsequently glued to the vibratome stage. Tissue was then sliced into 300 µm sections and plated onto 0.4 µm pore size hydrophilic polytetrafluoroethylene (PTFE) membrane inserts (Millipore Sigma) (see Figure 2.1). One to three tumour slices were plated onto each insert which sat in a 6-well culture dish. The slices were maintained in neurobasal supplemented with

0.01 M N-2-hydroxyethylpiperazine-N-2-ethane sulfonic acid (HEPES) 1% PSQ, and 1X B-27 supplement (Thermo Fisher Scientific). This media was added to the bottom of the well to allow it to be taken up by the slice through the membrane. After 24 hours the media was collected for extracellular vesicle analysis, and the organotypic slices were transduced with lentivirus as described below. Media was then collected and replaced with fresh medium every 48 hrs for 10 days.

Figure 2.1. Diagram of organotypic slice culture of patient derived GBM slices. A Slices were cultured in a 6-well culture dish on 0.4 μm polycarbonate inserts. Media was added to the bottom of the well where it would be taken up by the slices through the membrane by diffusion. **B** Representative image of organotypic slice culture of patient derived GBM sample attached to cell culture insert membrane.

A

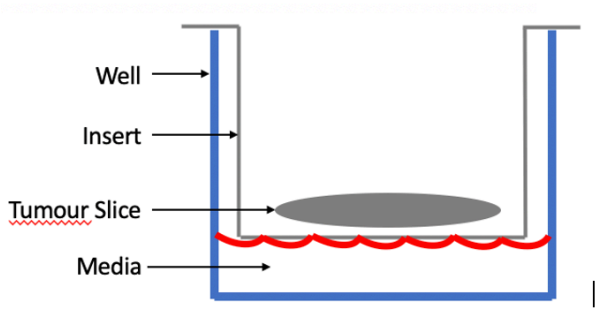

B

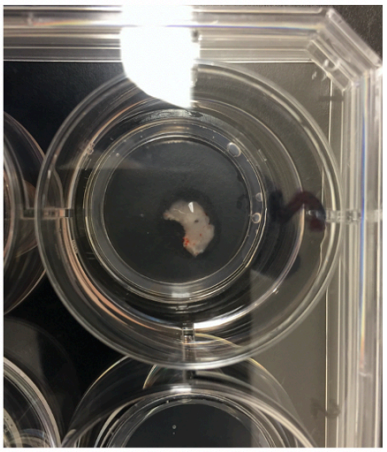

2.3 Plasmids and Cloning

A far-red fluorescent iRFP-PLJMI vector was designed and cloned by Dr. Kathleen Attwood and Inhwa Kim. Briefly, the iRFP760 gene of the pNLS-iRFP670 plasmid (Addgene #45466) was cloned into the PLJM1-empty backbone (Addgene #91980). Sequencing verification of the plasmid was done by Genewiz (Plainfield, New Jersey).

2.4 Recombinant Lentiviral Production

HEK 293T cells were utilized as a packaging cell line for the production of lentivirus using a second-generation lentiviral system as outlined in Figure 2.2 Cells were seeded to reach approximately 70-80% confluency on the day of transfection. Two µg of pSPAX2 (viral packaging, Addgene plasmid #1226) 1 µg of pMD2G (viral envelope, Addgene plasmid #12259) plasmids, and either 3.3 µg of iRFP-PLJM1 or empty vector PLJM1 (see section 2.3) was mixed with 500 µL of opti-MEM (Thermo Fisher Scientific). Separately, 18 µg polyethyleneimine (PEI, Sigma-Aldrich) was diluted in 500 µL opti-MEM. Plasmid and PEI solutions were then incubated separately for 5 min at room temperature. HEK293T cells were washed with PBS before addition of serum-free DMEM. PEI and plasmid solutions were then combined, incubated for 15 min at room temperature, and added dropwise to HEK-293T cells containing serum-free DMEM. Six hours post-transfection, the media was changed to DMEM supplemented with 10% HI-FBS and 1% L-Glutamine (Thermo Fisher Scientific). After 48 hrs, virus-containing supernatants were harvested and filtered through 0.45 µm polyethersulfone filters (VWR) before being aliquoted and stored at -80 °C. For concentrated lentiviral vectors, following filtration, the lentiviral supernatants were overlaid on top of a 20% sucrose cushion (20% w/v sucrose, 150mM sodium chloride (NaCl), 0.5 mM ethylenediaminetetraacetic acid (EDTA), 50 mM Tris Sigma

Aldrich) and centrifuged at 39k revolutions per minute (RPM) for 2 hours in a Beckman-Coulter Optima L-90K ultracentrifuge (Beckman-Coulter). The lentiviral pellet was then resuspended in either DMEM or neurobasal to achieve a 10X concentration.

Figure 2.2 Lentivirus production and concentration. A second-generation lentiviral system was employed to produce iRFP-PLJM1 expressing or PLJM1 empty vector lentivirus. HEK293T carrier cell line was transfected with pMD2G, pSPAX, and iRFP-PLJM1 plasmids. Forty eight hours post-transfection, the supernatant was collected and ultracentrifuged at 39K RPM for 2 hours. The viral pellet was then resuspended in media (DMEM or brain slice) to achieve 10X concentration, aliquoted and stored at -80°C for future titration and transduction.

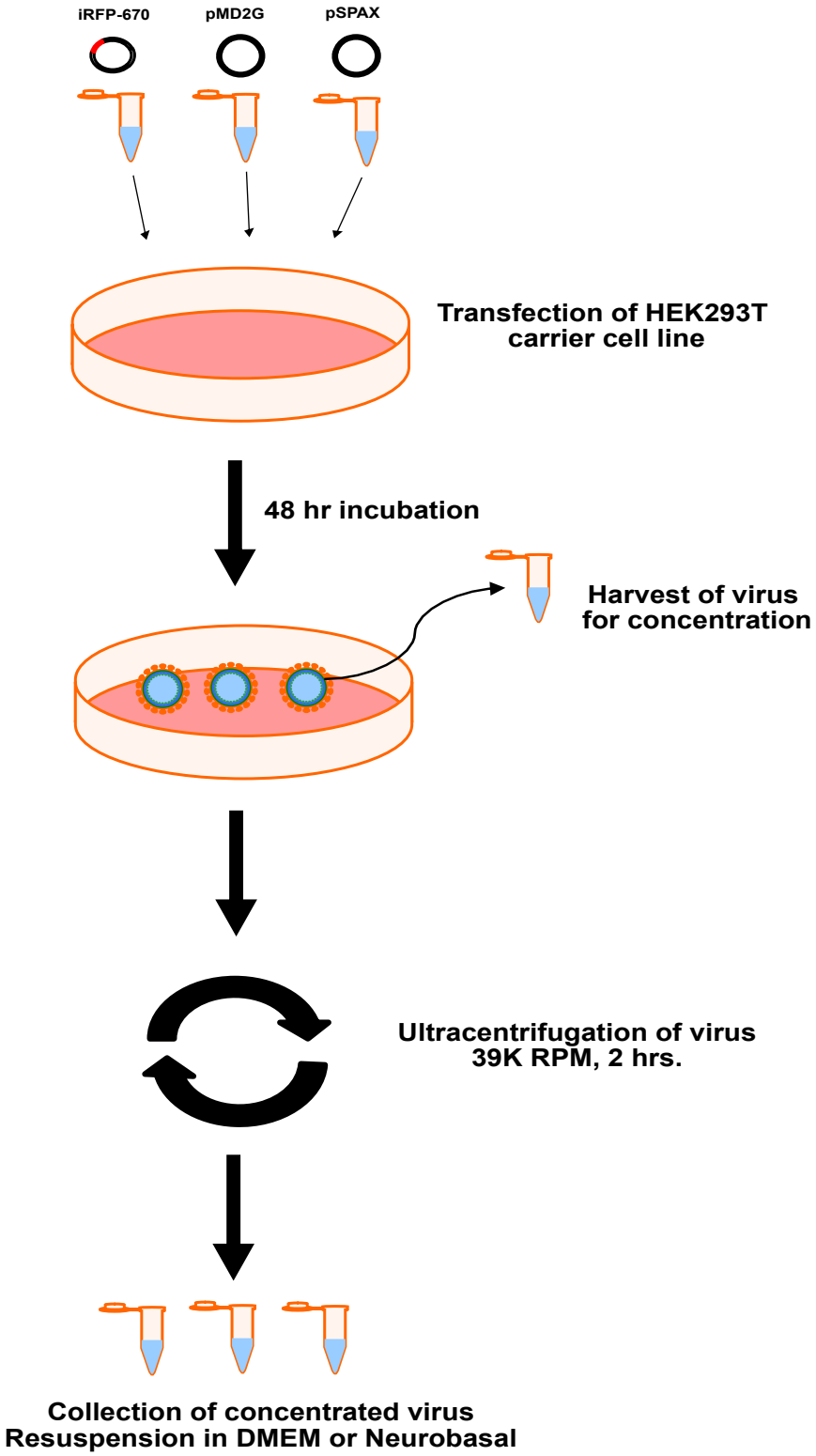
iRFP-670
pMD2G
pSPAX
Transfection of HEK293T
carrier cell line
48 hr incubation
Harvest of virus
for concentration
Ultracentrifugation of virus
39K RPM, 2 hrs.
Collection of concentrated virus
Resuspension in DMEM or Neurobasal

2.5 Lentiviral Titration

2.5.1 Functional Lentiviral Titration

Lentiviral vectors were titrated as described in Kutner et al. (2009), with the following adjustments. U251 cells were plated at a density of 30,000 cells/well to reach a low confluency of 20-30% the following day. Cells were then transduced with far-red fluorescent lentiviral vector or empty-vector control at varying dilutions (1:25, 1:50, 1:100, 1:125, 1:150, 1:175, 1:200, 1:300, 1:350) using 5 µg/mL of polybrene (company). Following 24 of transduction, cells were selected with 1 µg/mL puromycin (company) for 48 hrs and were imaged using EVOS FL Cell Imaging System (Thermo Fisher Scientific). Cells were harvested and viability assessed with fixable viability dye (FVD) eFluor450. Cells were then analyzed using the FACS CANTOII (BD Biosciences) cytometer for far-red fluorescence and eFluor 450 fluorescence to determine the percentage of cells infected with far-red fluorescent lentivirus. This percentage was then used to calculate titer in the form of transducing units (TU) per mL (TU/mL). This was done using the following formula, where F = % fluorescent cells, N = number of cells at time of transduction, D = fold dilution of vector sample used for transduction, and V = volume of lentivirus added to each well (µL) (Kutner et al., 2009):

$$\frac{TU}{mL} = \frac{(F)(N)(D)1000}{V}$$

2.5.2 Physical Lentiviral Titration

Lentiviral physical titration was carried out using a qPCR Lentivirus Titer Kit (ABM LV900) according to the manufacturer's instructions. Briefly, following lentivirus harvesting and concentration, the viral supernatant was lysed using viral lysis buffer and incubated at room temperature for 3 min. Following lysis, each sample was combined with GoTaq Master Mix 2X (Promega, A200A), and ABM reagent mix into a 96 well plate and sealed. Two standards were used as provided in the kit to generate a standard curve, and a no-template control of RNase-free diH_2O was included. qRT-PCR was run using the following program: a 20 min 42°C reverse transcription step and a 10 min 95°C enzyme activation step, followed by 30 cycles of 15 sec 95°C denaturation and 60 sec 60°C annealing/extension using the CFX Connect Real-Time PCR Detection System (BIO-RAD). C_t values were analyzed to determine lentiviral titer using the following formula:

$$\frac{infectious\ units}{mL} = e^{(Ct-b)/m}$$

Where m = slope of trend line, and b = y-intercept of trend line. Trend line generated using serially diluted DNA controls provided by ABM.

2.6 Lentiviral Transduction of Organotypic Slices

Transduction efficacy of the iRFP670-pLJM1 lentivirus was first confirmed in U251 immortalized and U3024 and U3085 primary cell lines prior to use on human tissue. Transduction was performed similarly to section 2.5 with the following adjustments: (state the # cells, density and dilutions). Following successful transduction in multiple cell lines, the iRFP670-pLJM1 or pLJM1 empty vector lentivirus was used to transduce the patient-derived GBM organotypic slices (see section 2.2). After 24 of culture, the slice culture medium was

replaced with a 1:2 dilution of lentivirus (iRFP-pLJM1 or empty-PLJM1 control) by addition into the bottom of the well below the membrane containing the tumour slice. Fifty microliters of virus-containing or control media (no virus) was also added to the top of the slice (see Figure 2.1). After 48 hours, the media was collected for extracellular vesicle (EV) analysis and replaced with regular neurobasal every 48 hrs for 9 days, for a total of 10 days in culture. Following the culture period, the slices were dissociated for flow cytometry analysis or fixed and mounted for confocal microscopy (see sections 2.7 and 2.8 respectively).

2.7 Confocal Microscopy

Tumour slices were fixed on the membrane insert in 4% paraformaldehyde (PFA) (Electron Microscopy Sciences) in 1X PBS for 4-5 hrs at 4 °C. Following fixation, slices were removed from the inserts by forceps and mounted onto microscopy slides using Prolong Gold (Thermo Fisher Scientific) and imaged on a Zeiss 710 Confocal Laser-Scanning Microscope (Zeiss International) in the Cellular and Molecular Digital Imaging Facility (CMDI) at Dalhousie University. Acquisition was carried out using consistent intensity measurements set to a laser intensity of 30% in the FAR-RED channel at 10X magnification (633nm laser, 638-747nm filter set). Gain, digital gain, and digital offset were set to 703, 0.30, and -4.69, respectively and kept consistent throughout experimental runs. To visualize lentiviral penetration of the slices, far-red fluorescence was imaged at multiple sectional planes through the slices at an interval of 4 μm, and z-stack images were generated using the Zeiss ZEN 3.2 software. Post-acquisition image analysis was done using ImageJ Software.

2.8 Flow Cytometry

2.8.1 Flow Cytometry of Immortalized Cellular Culture

Cells were plated at 75,000 cell/well and transduced after 24 hrs using far-red expressing lentivirus and empty vector control virus. After 48 hours in culture, cells were dissociated and pelleted by centrifugation at 1500 RPM for 5 minutes in an Eppendorf 5425 centrifuge (Sigma Aldrich), washed twice with 1X PBS and underwent staining procedure as specified below.

2.8.2 Flow Cytometry of Organotypic Slice Culture

Following 10 days in culture and 9 days of transduction, slices were washed with 1X PBS, removed from the insert and suspended in 500 μL collagenase (Thermo Fisher). The suspended slice was then incubated at 37 °C rocking at 75 RPM for 20 min, and were gently mechanically agitated by pipette. This process was repeated until the slice had completely dissociated (after approximately 60 total min rocking at 37 °C). The cell suspensions were then analyzed by hemocytometer for satisfactory single cell dissociation and filtered through a 70 μm cell strainer to remove debris and clumped tissue. Following filtration, cell suspensions were centrifuged for 5 min at 1500 RPM and resuspended in 1X PBS. Single colour controls consisted of iRFP-PLJM1 lentivirus transduced U251 cells for APC, heat kill controlled dissociated GBM slices (10 minutes at 65°C) for pacific blue, and non-transduced U251 cells stained with anti-GFAP Alexaflour 488 antibody (Thermo Fisher Scientific). The slices were then stained using FVD eFluor450 (Thermo Fisher Scientific) at 4°C for 30 min protected from light, washed twice with PBS and centrifuged at 1500 rpm for 5 min. Cell suspensions were fixed with 4% PFA for 10 min at room temperature with constant inversion, and permeabilized using 0.01% Triton X-100 (Sigma Aldrich) for 5 min at room temperature with constant inversion. Cell suspensions

were washed twice with FACS wash buffer (FWB) (PBS, 1% BSA, 0.1% sodium azide) before being incubated at 4 °C protected from light with anti-GFAP Alexafluor 488 antibody at 1 µg/mL (Thermo Fisher Scientific cat # 53-9892 -82) in FWB for 1 hour. Slices were then washed twice with FWB and resuspended in FACS buffer (0.5 % BSA, 2 mM EDTA, 1X PBS). Cells were analyzed using the BD FACS CANTOII flow cytometry, with automated compensation calculated using single colour positive controls by the FACSDIVA software (BD Biosciences). Cells were first gated using forward (FSC) and side (SSC) scatter measurements, and subsequently gated for viability (eFluor450 negativity; pacific blue channel), and the iRFP and GFAP positivity using APC and FITC channels respectively. Post-acquisition analysis was completed using FlowJo (BD Biosciences Company, San Jose California) and Flowing 2 software (Perttu Terho, Turku Centre for Biotechnology).

$$\frac{TU}{mL} = \frac{(F)(N)(D)1000}{V} \frac{infectious\ units}{mL} = e^{\frac{Ct-b}{m}}$$

2.9 Extracellular Vesicle Analysis

Organotypic GBM slices were cultured as outlined above (section 2.2). Twenty-four hours into culture during the first media change, media was collected from the bottom of the well. The media was frozen at -80 °C and stored for subsequent shipment to the Atlantic Cancer Research Institute (ACRI) for analysis in the lab of Jeremy Roy. Analysis was conducted as outlined by Ghosh et al. (2014). Briefly, media samples were thawed and cleared by centrifugation at 17,000 xg and incubated overnight with Vn96 peptide (New England Peptide, Gardner, US, US Patent # 8,956,878) at 4°C. This peptide which binds heat shock proteins on the surface of EVs and precipitates EVs out of solution allows for isolation of EVs in both biological

fluids and culture media. ACRI conducted analysis of the Vn96-captured EVs from conditioned culture media using western blot and nanoparticle tracking analysis for binding of canonical EV markers and presence and counts of EV-sized particles, respectively. ACRI further conducted nanoflow cytometry on media samples without the use of Vn96 capture.

2.10 Statistical Analysis

Statistical analysis was carried out using GraphPad PRISM and Microsoft Excel software to calculate statistical differences. Statistical tests to compare replicates of biological independent experiments where appropriate were one-way analysis of variance (ANOVA) with multiple comparisons and one-way unpaired t-tests. Statistical significance was denoted if $p < 0.05$.

CHAPTER 3 RESULTS

3.1 Generation of Organotypic Slice Culture Model of GBM

We aimed to generate a patient derived organotypic slice culture of GBM that could be further utilized to model various aspects of GBM biology.

Patient derived tumours were sliced to 300 μm thick slices cut on a vibratome and cultured in brain tumour media (see **Chapter 2. Methods)**. Our first goal was to establish viability of our culture system. To determine slice viability, two methods were employed, which were slice adherence and spreading on the membrane, and FVD efluor450. Humpel et al., (2015) utilized slice adherence to the diffusion membrane and subsequent spreading as a test of viability. Non-viable slices will not attach to the membrane. **Figure 3.1.1 A** demonstrates one of our representative slices adhering to the membrane in culture. Figure **3.1.1 B** demonstrates cellular spreading by light microscopy in a viable section as opposed to a non-viable slices where cellular spreading was not observed **(Figure 3.1.1)**. However, due to the subjective and qualitative nature of slice adherence as a determination of slice viability, more quantitative viability analysis was undertaken using cellular viability dye FVD efluor 450 followed by FACS analysis. Dissociated slices were stained with FVD efluor 450 dye, fixed and analysed by flow cytometry. Efluor viability dye enters the membrane of dead cells binds amino groups in the cytosol, therefore is positive in dead cells. By FACS analysis our GBM slices maintain viability for at least 10 days, with a **(Figure. 3.1.1**) mean viability following 10 days of culture of 77% ± 10.1 (n=4). We also cultured slices from non-cancerous brain tissue taken during cortex resection for treatment of epilepsy. This cortex acquired during surgery for the treatment of epilepsy had a slightly higher 10-day viability by FVD Efluor analysis at 88% (n=2), although this was not statistically significant and may be explained by low numbers. **(Figure 3.1.1)**. One non-

astrocytoma tumour, ependymoma, was cultured and analyzed and showed a significantly reduced viability of 40% after 10 days **(Supplemental Figure 1).**

Figure 3.1.1. Organotypic GBM slice cultures stay viable for 10 days in culture. GBM slices were culture for 10 days, dissociated and stained for eFluor450 and analyzed by flow cytometry. **(A)** Representative image of organotypic brain tumour slices in culture adhering to membrane. Arrow indicates slice. **(B)** Representative brightfield microscopy of organotypic GBM slice adhering to membrane (left panel) and not adhering to membrane (right panel). Dotted line indicates border of slice, with arrows indicating examples of spreading cells (right panel). **(C)** Representative flow cytometry gating strategy. Cellular debris was excluded by forward scatter area and side scatter area (left panel) and doublets were excluded by scatter-width and side scatter-height (center panel). Cell viability was assessed by eFluor 450 negativity relative to single colour controls (right panel). **(D)** Quantification of flow cytometry analysis to determine percent viability by eFluor450 negativity at day 10. GBM (n = 4 biological replicates, data represented as mean ± SD) slice viability compared with cortex removed for epilepsy surgery (n = 2 biological replicates).

A

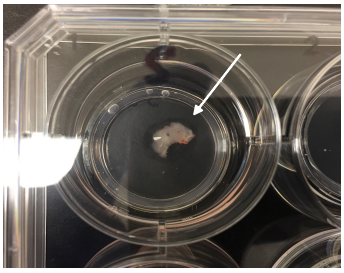

B

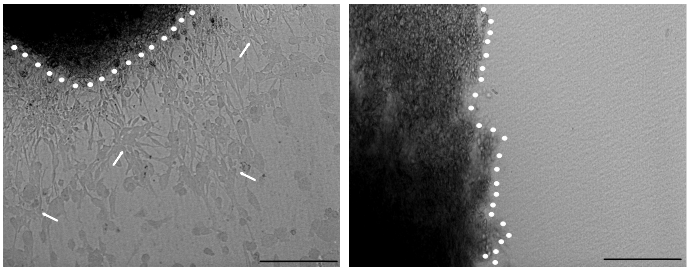
Viable
Non-Viable

C

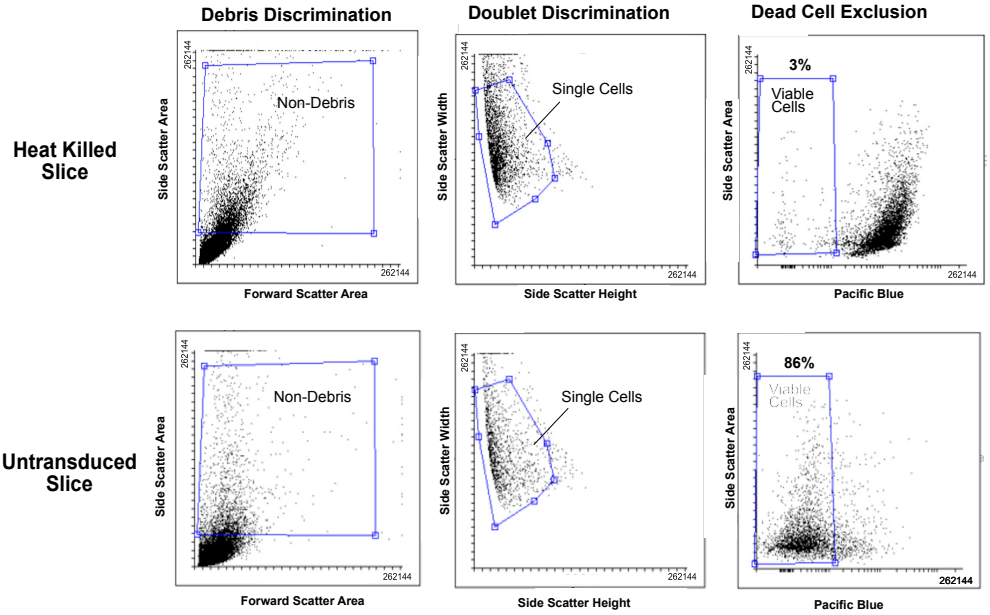
Debris Discrimination
Doublet Discrimination
Dead Cell Exclusion
Heat Killed Slice
Untransduced Slice
Non-Debris
Single Cells
3%
Viable Cells
86%
Side Scatter Area
Forward Scatter Area
Side Scatter Width
Side Scatter Height
Pacific Blue
262144

D

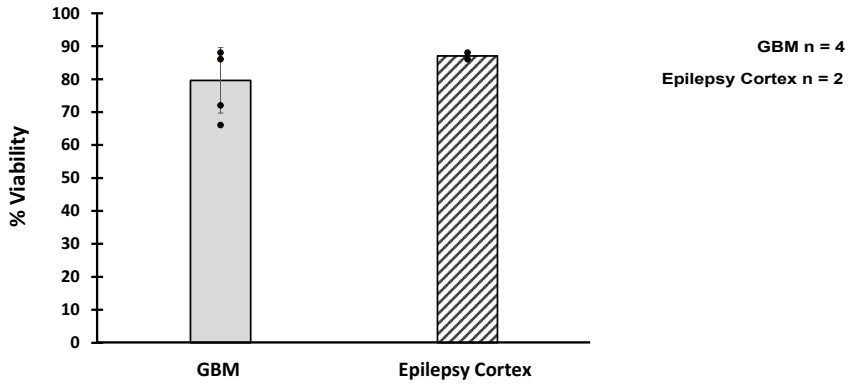
% Viability
100
90
80
70
60
50
40
30
20
10
0
GBM
Epilepsy Cortex
GBM n = 4
Epilepsy Cortex n = 2

3.2 Production, Concentration, and Titration of iRFP-PLM1 Lentivirus

Following establishment of a viable organotypic slice culture model, we then wanted to pursue a way to use the model to study GBM. We proposed genetically manipulating the slices with a far-red fluorescent lentiviral vector to confirm amenability of the slices for genetic manipulation. iRFP-expressing lentivirus and empty PLJM1 lentivirus was produced using HEK293T carrier cell line and concentrated 10X by ultracentrifugation **(Figure 2.2).** Unconcentrated lentivirus stocks were used to transduce U-251 MG immortalized cell lines (Figure 3.2.1 A) and primary cell lines U3024 (Figure 3.2.1 B) and U3085 (Figure 3.2.1 C). Both immortalized and primary cell lines exhibited far-red fluorescence as compared to empty vector transduced and non-transduced controls confirming functional lentiviral particles (Figure 3.2.1).

Figure 3.2.1. iRFP-670 expressing lentivirus induces far-red fluorescence in immortalized and primary GBM cell lines. Immortalized GBM cell line U-251 MG **(A)**, primary GBM cell line U3024 **(B)** and primary GBM cell line U3085 **(C)** were transduced at 1:100 viral dilution of both iRFP-670 expressing lentivirus (left panel) and empty vector control lentivirus (centre panel) along with no virus controls (right panel) then imaged 72 hours following transduction. Images were taken both using brightfield (top panel) and fluorescent (bottom panel) microscopy. Scale bars = 400 μm

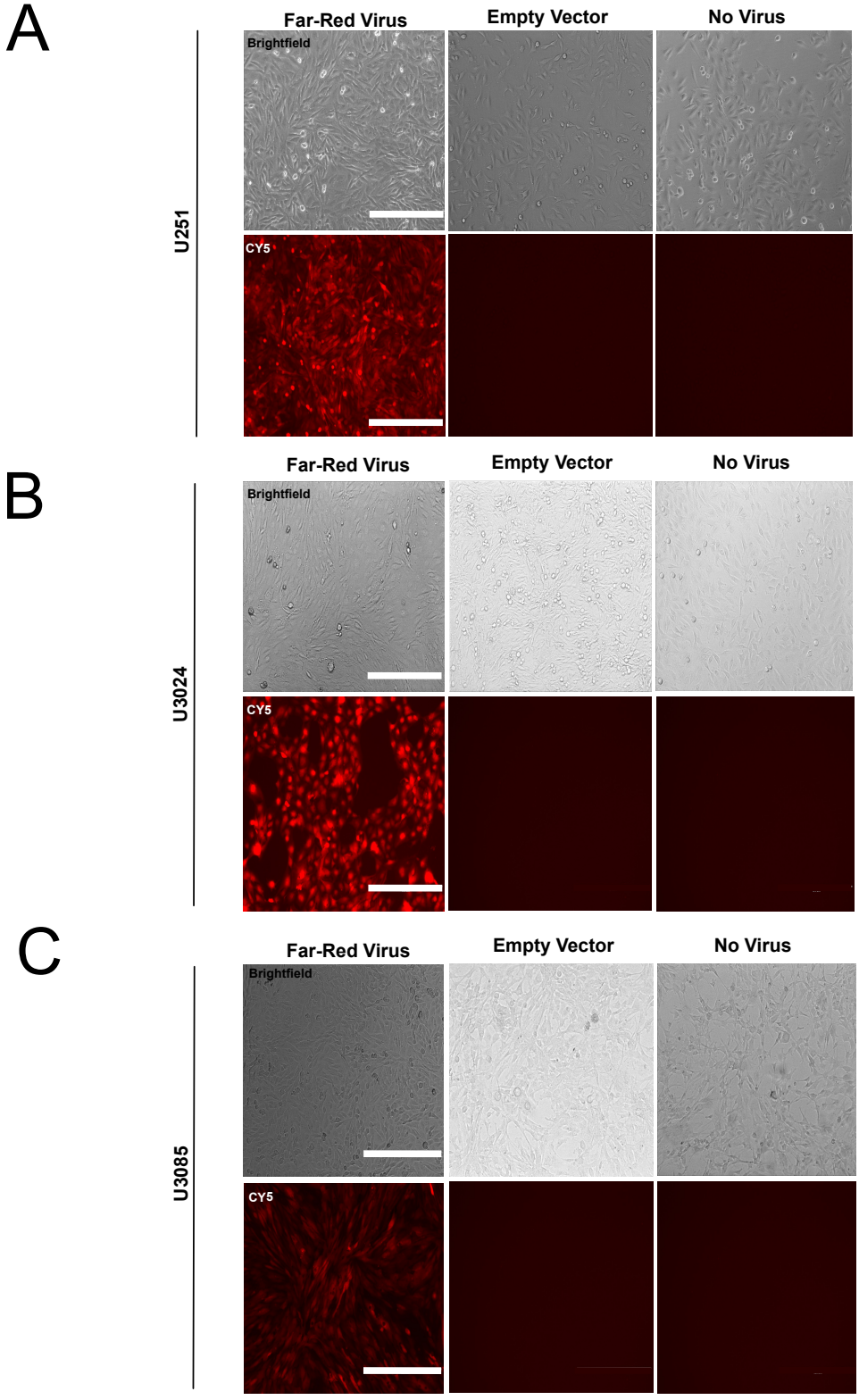
A
Far-Red Virus
Empty Vector
No Virus
Brightfield
CY5
U251
B
Far-Red Virus
Empty Vector
No Virus
Brightfield
CY5
U3024
C
Far-Red Virus
Empty Vector
No Virus
Brightfield
CY5
U3085

The far-red lentivirus is typically resuspended in DMEM after culture with HEK293T cells. The organotypic slices are maintained in neurobasal media without FBS. We were concerned that the volume of virus required for transduction would dilute the neurobasal medial and impair slice viability. We therefore performed a vehicle control experiment to determine the effect of adding 300ul of FBS/DMEM for 48 hours on GBM slice viability **(Figure 3.2.2).** Flow cytometry analysis using eFluor 450 dye demonstrated an approximately 50% drop in viability (from 80% to 40%, n=2) between slices cultured in standard conditions (neurobasal) and slices cultured and exposed to 300 uL DMEM for 48 hours (**Figure 3.2.2**). Thus, future steps to reduce slice exposure to DMEM were warranted and viral resuspension in neurobasal was carried out.

To determine if resuspension in neurobasal adversely affected lentiviral infectivity, lentiviral vectors resuspended in DMEM, neurobasal, and unconcentrated lentiviral vector were titrated onto U251-MG cells. Across 6 different dilutions, there was no significant functional difference between iRFP-expressing lentivirus resuspended in neurobasal and DMEM **(Figure 3.2.3).** Further quantification of the physical transducing units per millilitre (TU/mL) found no significant difference between lentivirus resuspended in neurobasal and DMEM **(Figure 3.2.3).** Thus, resuspension in neurobasal was deemed appropriate.

Figure 3.2.2. DMEM exposure results in reduced viability of organotypic GBM slices. Patient-derived organotypic slice cultures were treated normally with neurobasal or neurobasal with 300 μL DMEM. **A)** Representative flow cytometry analysis of viability in patient-derived GBM organotypic slice culture. Gating for live cells as previously described in Figure 3.1.1. **(B)** Quantification of slice viability based on flow cytometry analysis of eFluor450 staining. Data represented as means ± SD, n = 2 biological replicates

A

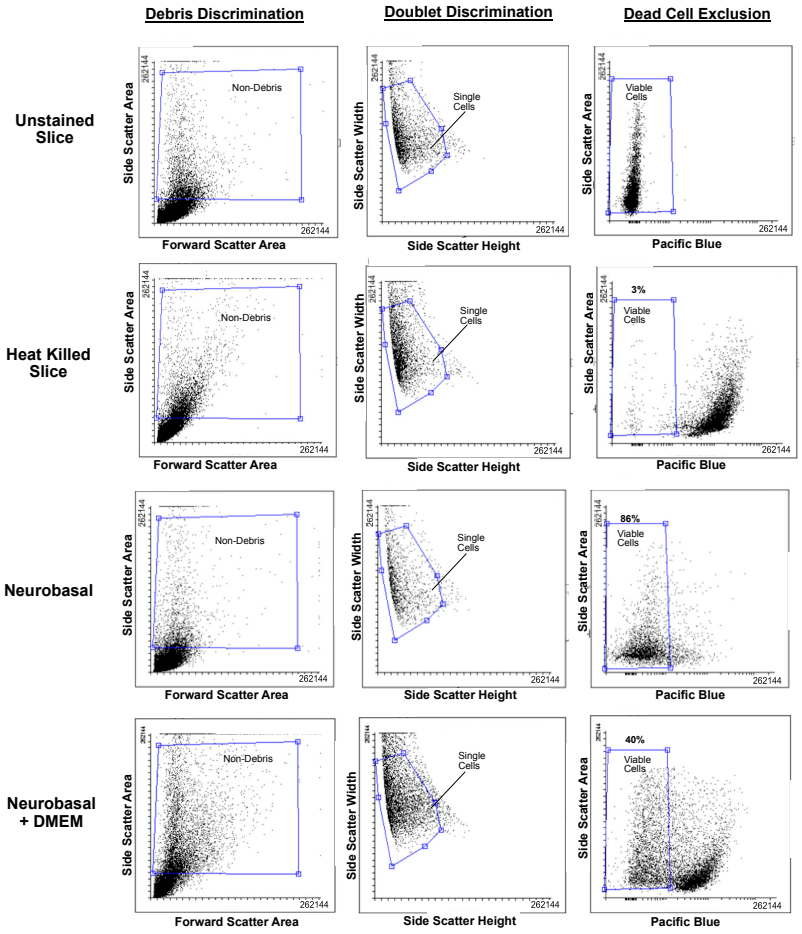
Debris Discrimination
Doublet Discrimination
Dead Cell Exclusion
Unstained Slice
Heat Killed Slice
Neurobasal
Neurobasal + DMEM
Non-Debris
Single Cells
Viable Cells
3%
86%
40%
Side Scatter Area
Forward Scatter Area
Side Scatter Width
Side Scatter Height
Pacific Blue
262144

B

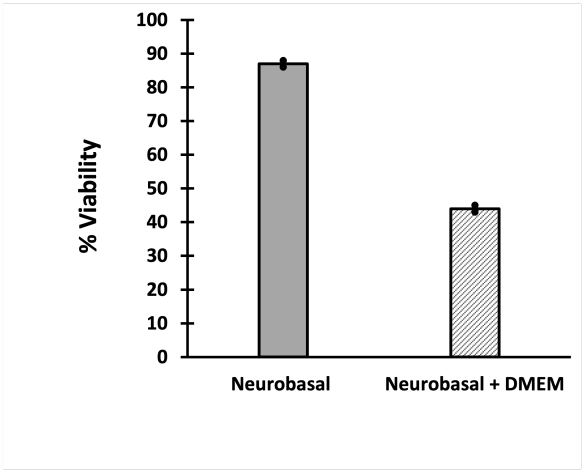
% Viability
100
90
80
70
60
50
40
30
20
10
0
Neurobasal
Neurobasal + DMEM

n = 2

To determine if resuspension in neurobasal adversely affected lentiviral infectivity, lentiviral vectors resuspended in DMEM, neurobasal, and unconcentrated lentiviral vector were titrated onto U251-MG cells. Across 6 different dilutions, there was no significant functional difference between iRFP-expressing lentivirus resuspended in neurobasal and DMEM **(Figure 3.2.3).** Further quantification of the physical transducing units per millilitre (TU/mL) found no significant difference between lentivirus resuspended in neurobasal and DMEM **(Figure 3.2.3).** Thus, resuspension in neurobasal was deemed appropriate.

Figure 3.2.3. Lentiviral transduction efficiency is not reduced when resuspended in neurobasal medium. U-251 MG glioma cells were transduced with concentrated iRFP-expressing lentivirus resuspended in DMEM or neurobasal at varying dilutions. **(A)** Representative flow cytometry analysis (1:100 dilution) to determine percentage of iRFP+ cells to calculate functional titration. **(B)** Brightfield and fluorescent microscopy of varying dilutions of each virus, with percentage iRFP+ determined by corresponding flow cytometry**.** Scale bars = 400 μm **(C)** Left panel: lentiviral vectors concentrated and resuspended in DMEM or neurobasal were functionally titrated as outlined by Kutner et al. (2009) and described in Materials and Methods. Functional titration values were averaged over 6 dilutions. Right panel: lentiviral vectors concentrated and resuspended in DMEM or neurobasal were analyzed using qPCR to determine physical titer.

A

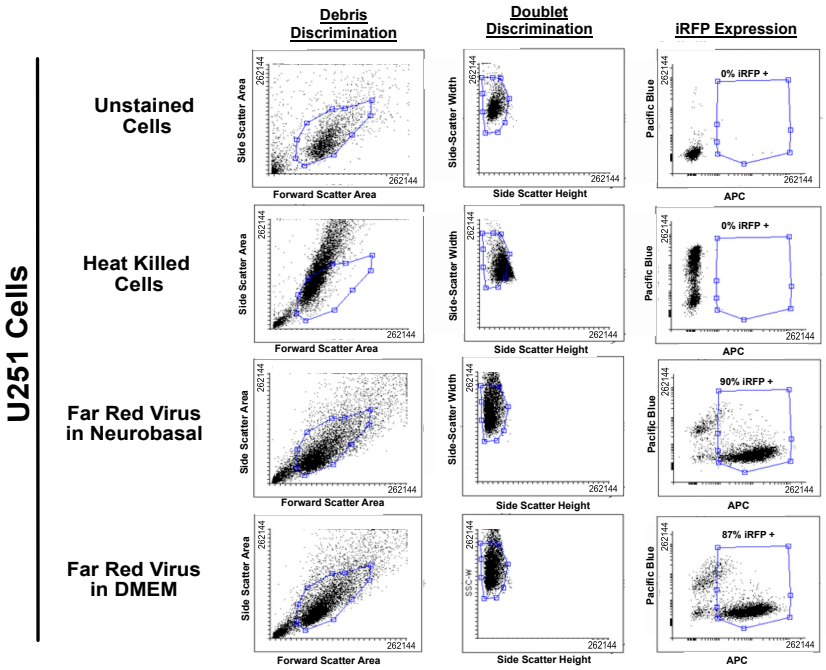
U251 Cells
Debris Discrimination
Doublet Discrimination
iRFP Expression
Unstained Cells
Heat Killed Cells
Far Red Virus in Neurobasal
Far Red Virus in DMEM
Side Scatter Area
Forward Scatter Area
Side-Scatter Width
Side Scatter Height
Pacific Blue
APC
0% iRFP +
90% iRFP +
87% iRFP +
262144

B

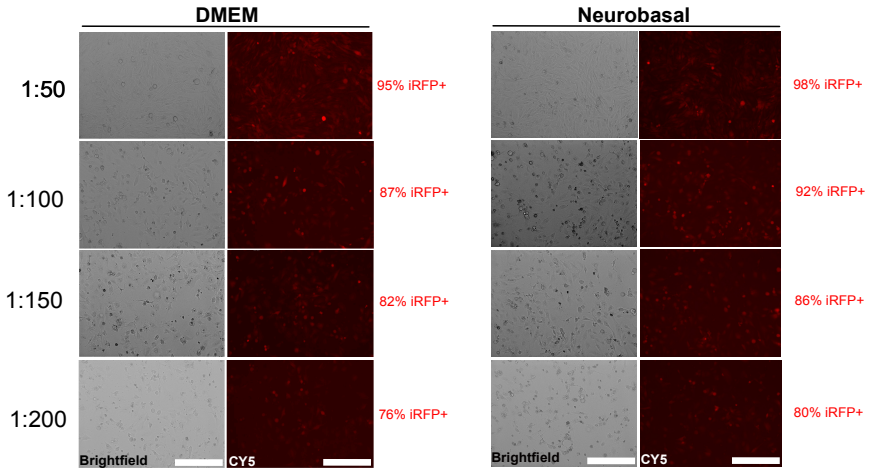
DMEM
Neurobasal
1:50
1:100
1:150
1:200
95% iRFP+
87% iRFP+
82% iRFP+
76% iRFP+
98% iRFP+
92% iRFP+
86% iRFP+
80% iRFP+
Brightfield
CY5

C

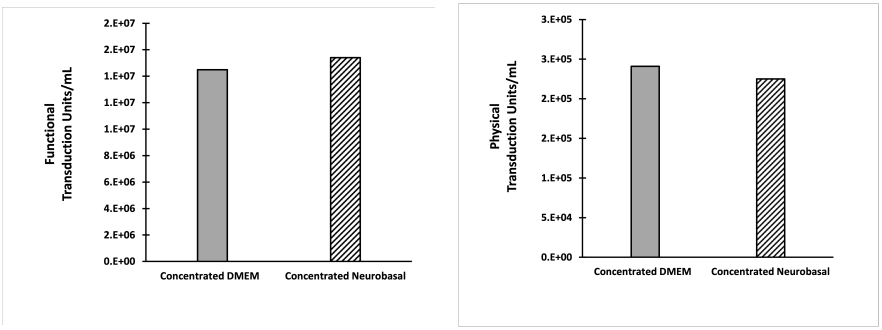
Functional Transduction Units/mL
2.E+07
1.E+07
8.E+06
6.E+06
4.E+06
2.E+06
0.E+00
Concentrated DMEM
Concentrated Neurobasal
Physical Transduction Units/mL
3.E+05
2.E+05
1.E+05
5.E+04
0.E+00

3.3. iRFP-PLJM1 Expressing Lentivirus Transduction of Organotypic Slice Cultures

Our organotypic GBM slice cultures were transduced 24 hrs following resection with the far-red fluorescent vector for 48 hours. Far-red fluorescence was observed at day 10 in culture by confocal microscopy (**Figure 3.3.1**). The fluorescent signal was analysed by image J and compared to empty vector transduced and non-transduced slices and approached statistical significance. Far-red fluorescence was viewed throughout the thickness of the slice compared to both no virus controls and empty vector controls by confocal microscopy **(Figure 3.3.1)**.

To further demonstrate far-red expression and to quantify far-red expression we employed FACS analysis. To determine the proportion of the slice being transduced, slices were dissociated and analyzed by flow cytometry. iRFP-expressing lentivirus transduced slices expressed 18 ± 4.8 %far-red fluorescence whereas no virus control and empty vector control expressed 5 ± 1.16 % and 4 ± 1.5 %far-red fluorescence, respectively **(Figure 3.3.2).**

We next wanted to know which cell type the lentivirus was transducing. As discussed above the GBM organotypic slice cultures contains many cell types. To demonstrate lentiviral transduction of the tumour and determine what cell type the virus was infecting, we employed the GBM cell marker GFAP, which showed significant GFAP positivity in all slices regardless of iRFP transduction, averaging 68 ± .5 % GFAP positive cells **(Figure 3.3.2).** Of the total population of cells, 16 ± 1.1 % of the GBM slices treated with iRFP-expressing lentivirus were iRFP/GFAP$^{+/+}$ whereas untreated GBM slices and empty vector treated GBM slices were 5 ± 0.5 % and 4 ± 0.7% iRFP/GFAP$^{+/+}$, respectively (**Figure 3.3.2).**

Figure 3.3.1. Organotypic GBM slices transduced with far red-expressing lentivirus show far-red expression throughout slice by confocal microscopy. GBM organotypic slices were transduced with far red-expressing lentivirus or empty vector lentivirus at 1:2 viral dilution for 48 hr. (**A)** Top: Representative brightfield and fluorescent images of GBM organotypic slices. Slices were fixed and imaged for far-red fluorescence by confocal microscopy, axis representing images being viewed along z-axis from top of slice. Bottom: Representative 3D projections of confocal z-stack of GBM organotypic slices viewed along the y-axis **(B)** Fluorescence was quantified by ImageJ for fluorescence by mean gray value and analyzed by fold change over untransduced. Data is presented as the means of technical and biological triplicates ± SD, one-way ANOVA for multiple comparisons. Scale bars = 400 μm

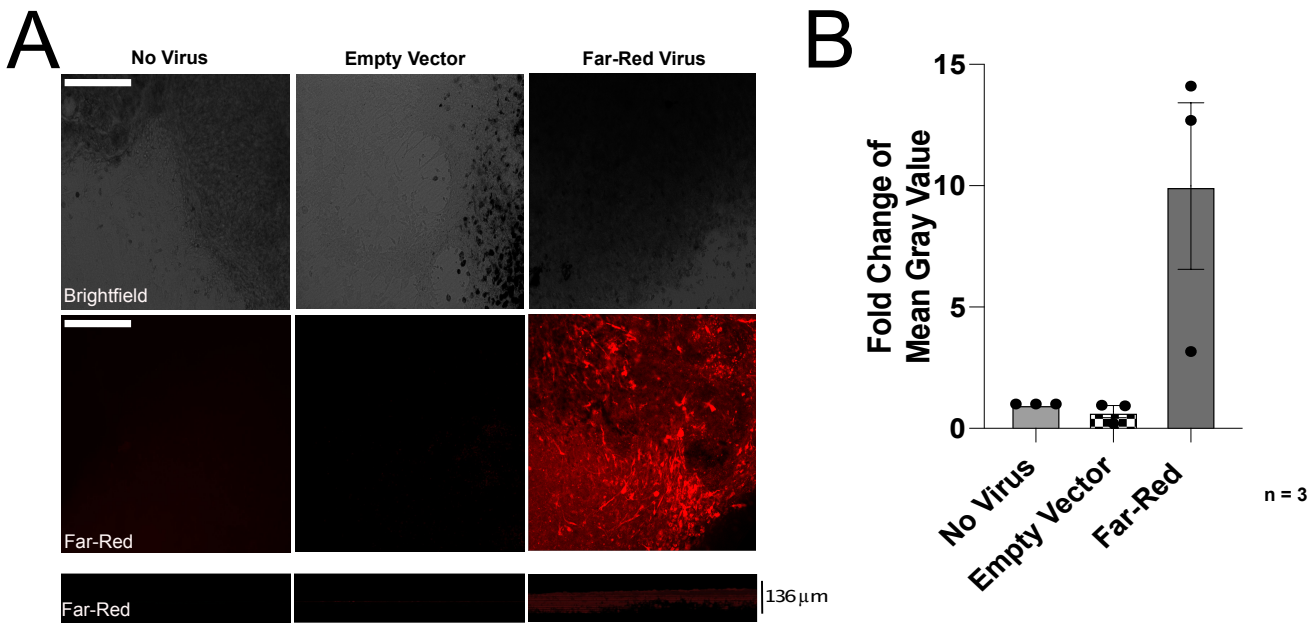
A
No Virus
Empty Vector
Far-Red Virus
Brightfield
Far-Red
Far-Red
136 µm
B
Fold Change of Mean Gray Value
15
10
5
0
No Virus
Empty Vector
Far-Red
n = 3

Figure 3.3.2. Organotypic GBM slices transduced with far red-expressing lentivirus show far red expression in 18% of slice and far red/GFAP expression in 15% of the slice.
GBM organotypic cultures were transduced using 10X concentrated iRFP-expressing lentivirus and 10X concentrated empty-vector control virus for 48 hours. **(A)** Representative dot plots of analysis of far-red fluorescence (APC). Gating for viable cells to include in fluorescent analysis conducted as described previously (Figure 3.3.1). Fluorescent parameter gating to determine threshold done using single-colour controls (see bottom right inset). **(B)** Top panel: Quantification of percentage of far red+ cells in no virus, empty vector, and far red-expressing lentivirus transduced GBM slice cultures (top and bottom right quadrants). Middle panel: quantification of GFAP+ cells in no virus, empty vector, and far-red expressing lentivirus transduced GBM slices. (top right and left quadrants). Bottom panel: quantification of far-red/GFAP+ cells in no virus, empty vector, and far-red expressing lentivirus transduced GBM slices. **(C)** Table outlining sample positivity for iRFP-expressing lentiviral transduction, GFAP positivity, and simultaneous for iRFP-expressing lentiviral transduction and GFAP positivity. Samples acquired from two female patients and one male patient. Data represented as means of biological replicates ± SD, unpaired, one-tailed t-test* $p< 0.05$; ***$p<0.001$, ns = not significant

A

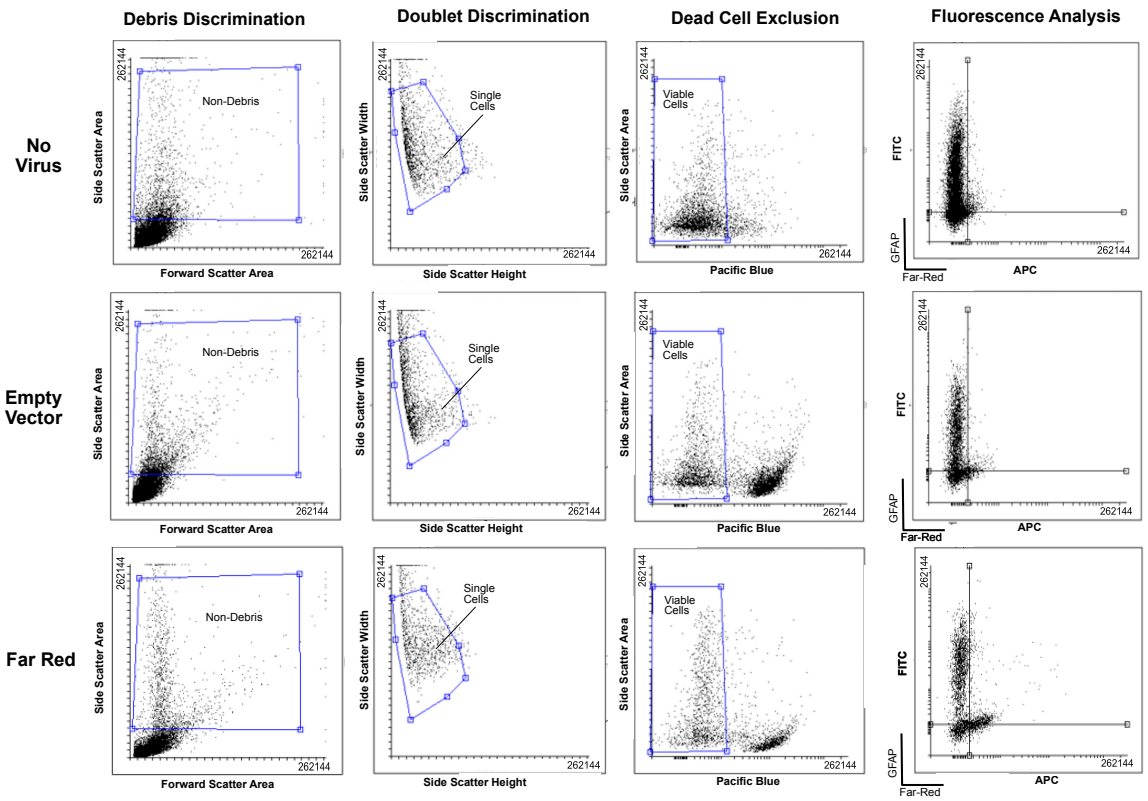

B

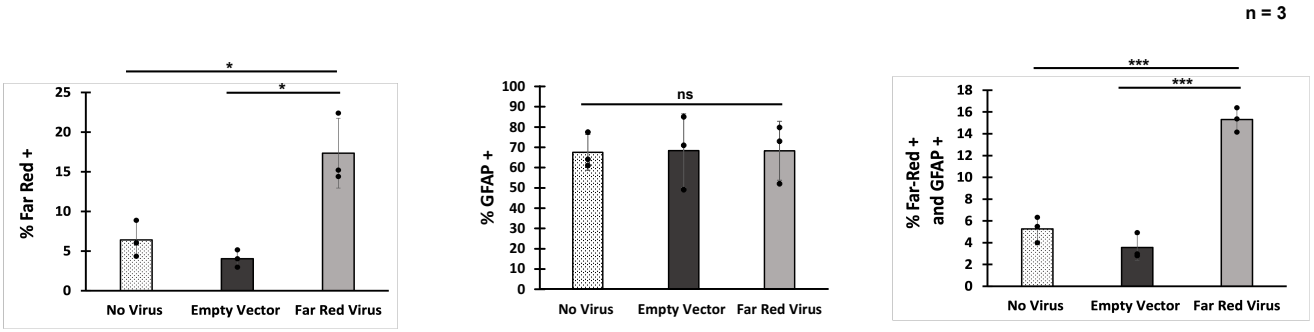

C

	%FarRed+	%GFAP+	%FarRed+/GFAP+
No Virus	6.4 ± 2.2	67.5 ± 8.7	5.2 ± 1.1
Empty Vector	4.0 ± 1.1	68.3 ± 18.3	3.5 ± 1.2
Far Red Virus	17.3 ± 4.4	68.2 ± 14.4	15.3 ± 1.1

3.4 Isolation of Extracellular Vesicles from Organotypic Slice Culture Model

Our laboratory has recently begun investigating EVs in GBM pathobiology. We sought to determine whether our GBM organotypic cell culture model could potentially be used to model GBM EV biology. We asked whether the GBM conditioned media expressed typical markers of EVs. To determine whether or not the organotypic slice culture model of GBM developed in this project could also be utilized to study GBM-derived EVs, conditioned culture media (CCM) of untreated GBM slices 24 hours following resection was collected and analysed by our collaborators at the ACRI; Dr. Jeremy Roy and Catherine Taylor. Media was processed for EV analysis by Vn-96 capture which binds heat shock proteins on the membrane of EVs and forms precipitates that can then be analyzed (Ghosh et al., 2015). Vn-96 captured EVs from media samples were analyzed by nanoparticle tracking analysis and found each patient sample analyzed contain significant number of particles of the correct size typical of culture media **(Figure 3.4.1 A).** Vn-96 captured EVs were then analyzed for canonical EV markers as set out by MISEV (2018) to be field standard. Vn-96 captured EVs analyzed by western blot show presence of EV markers CD63, HSP70, and FLOT1, and negativity for contamination marker CANX **(Figure 3.4.1 B).**

To further determine if the CCM shows positivity for EV markers, both pooled individual media were probed for CD9, CD63 and GD2 using nanoflow cytometry. Pooled media from six separate brain tumours showed positivity for CD63 and GD2 over non-conditioned media control **(Figure 3.4.2 A)**. Furthermore, analysis of individual tumour media samples showed varying levels of CD63 and GD2 expression **(Figure 3.4.2 B).**

Figure 3.4.1. Organotypic GBM slice-conditioned culture media have EV-sized particles and expression of canonical EV markers. Following 24 of culture, the media of untreated GBM slices was collected, processed using Vn96 EV capture and analyzed for EVs numbers, size, and markers. **(A)** Nanoparticle tracking analysis (NTA) for size and quantity in of particles in GBM organotypic slice culture media. **(B)** Western blotting for EV markers CD63, HSC70, FLOT1, and negative control CANX of Vn96 captured EVs from media of GBM organotypic slice cultures. Analysis conducted by ACRI.

A

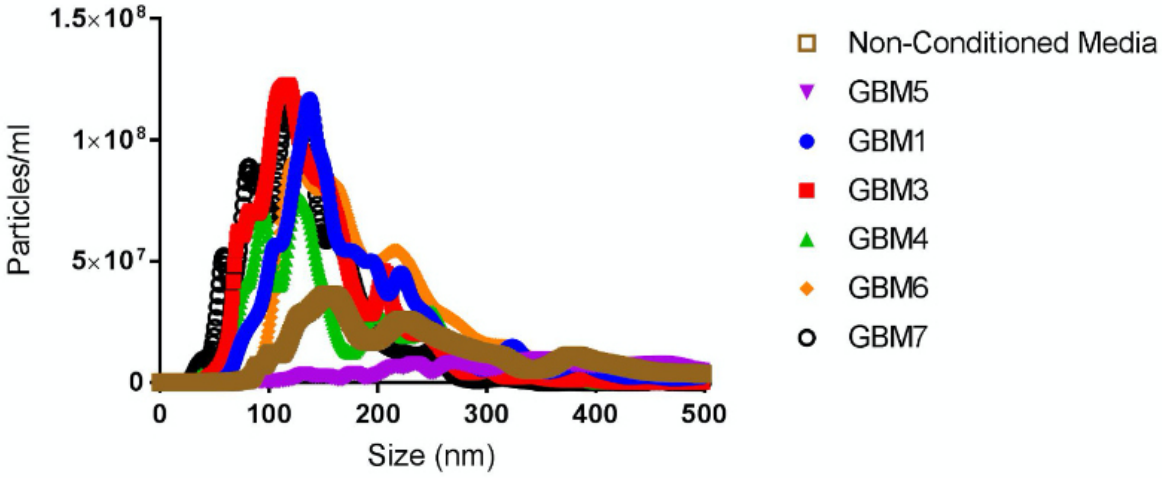
1.5×10^8
1×10^8
5×10^7
0
Particles/ml
0
100
200
300
400
500
Size (nm)
Non-Conditioned Media
GBM5
GBM1
GBM3
GBM4
GBM6
GBM7

B

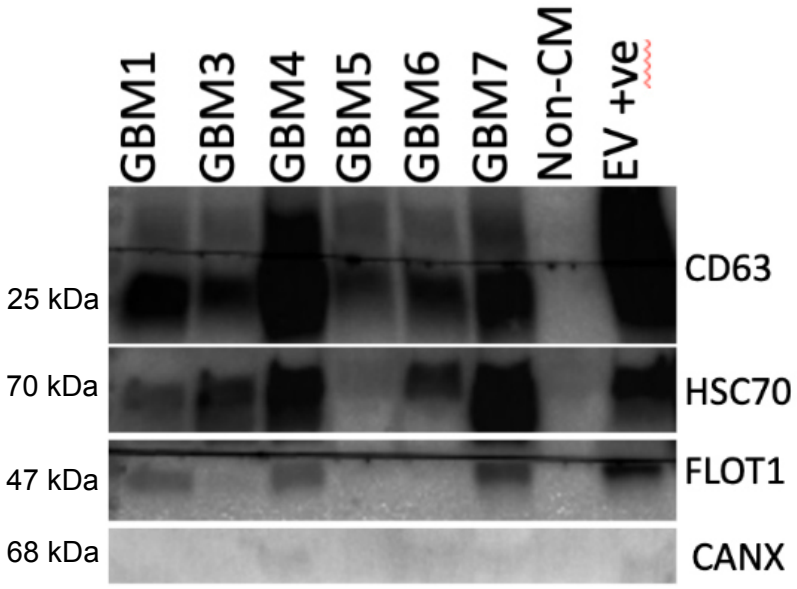
GBM1
GBM3
GBM4
GBM5
GBM6
GBM7
Non-CM
EV +ve
25 kDa
CD63
70 kDa
HSC70
47 kDa
FLOT1
68 kDa
CANX

Figure 3.4.2. Pooled and individual organotypic GBM slice-conditioned culture media are positive for canonical EV marker CD63. Following 24 of culture, the media of untreated GBM slices was collected and analyzed for EV markers. **(A)** nanoFC analysis of pooled organotypic slice culture media for EV markers CD63 and CD9, and CNS tumour marker GD2. **(B)** nanoFC analysis of individual tumour samples for EV marker CD63 and CNS tumour marker GD2. Data represented as percent positive events normalized to total events. Analysis conducted by ACRI.

A

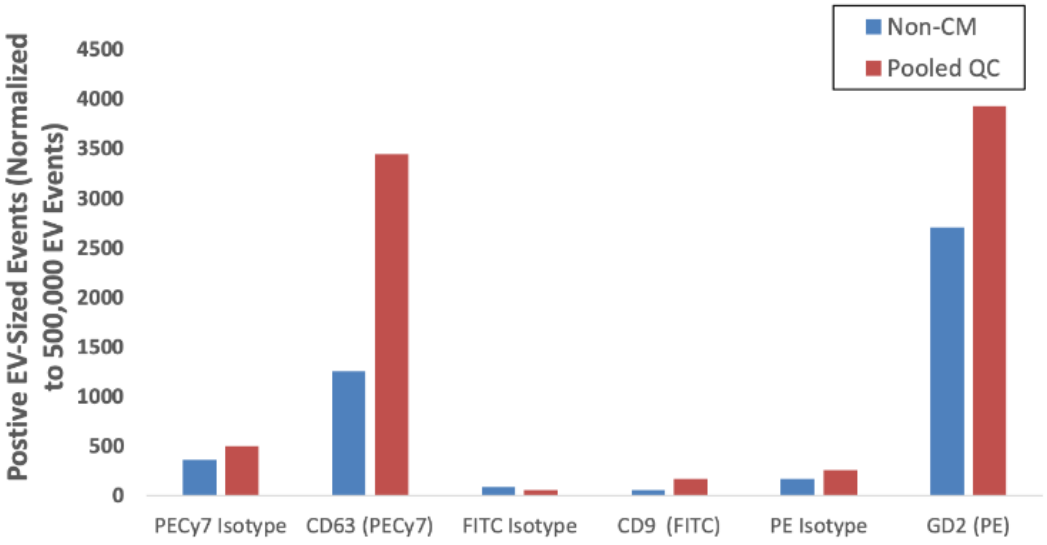
Non-CM
Pooled QC
Postive EV-Sized Events (Normalized to 500,000 EV Events)
4500
4000
3500
3000
2500
2000
1500
1000
500
0
PECy7 Isotype
CD63 (PECy7)
FITC Isotype
CD9 (FITC)
PE Isotype
GD2 (PE)

B

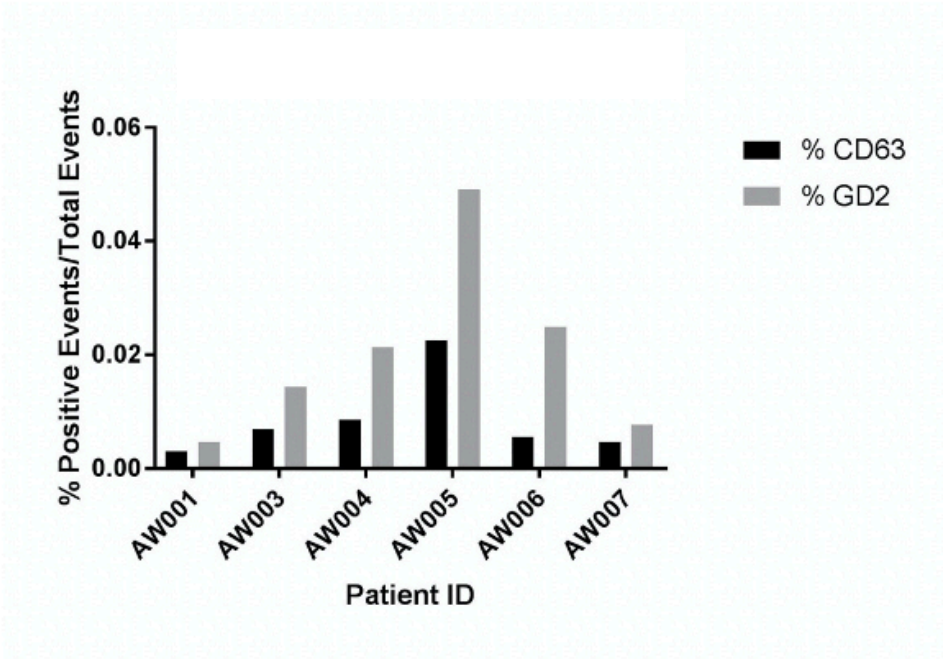
% CD63
% GD2
% Positive Events/Total Events
0.06
0.04
0.02
0.00
AW001
AW003
AW004
AW005
AW006
AW007
Patient ID

CHAPTER 4 DISCUSSION

4.1 Establishing Viable Organotypic Slice Culture Model of GBM

GBM is a highly malignant tumour with a complicated, heterogenous TME. This TME and the heterogeneity within contribute significantly to GBM's inevitable recurrence. We aimed to add patient-derived organotypic slice culture as a viable genetically manipulable model system in the armament for researchers studying this devastating disease. An organotypic slice culture model hopes to supplement the current experimental models of GBM, which are predominantly monocultured immortalized cell lines, monocultured primary cell lines, and animal models (predominantly rodent). Cell lines and animal models have both benefits and drawbacks, as do all culture systems. Immortalized cell lines are valuable for generating preliminary data but suffer from genetic drift and lack the stromal context of GBM, and tumours that initiate upon xenotransplantation of immortalized cells into mice are histologically distinct from GBM (Lee et al., 2006; Robertson et al., 2010). Primary cell lines partly address the shortcomings of immortalized cell culture and can be grown either in monoculture or 3D neurospheres (Hammati et al., 2003; Singh et al., 2003; Galli et al., 2004; Pollard et al 2009). Importantly, primary cell cultures are established without genetic manipulations or selection and are therefore enable experiments that encompass the original genetic heterogeneity of the tumour (Robertson et al., 2019). Animal models, which are typically mouse models, are the gold standard in GBM research as they best represent the *in-situ* environment of human GBM (Robertson et al., 2019). Such mouse models can be allographs, xenographs, or genetically engineered mouse lines (Schiffer et al., 1978; Ben-David et al., 2017).

In this study, we have further demonstrated the establishment of an ex-vivo organotypic slice culture model of GBM. We confirmed slice culture viability using two methods. Firstly,

slice viability was confirmed by visual inspection as described by Humpel et al., 2015. Viable slices both adhere to the porous membrane insert and exhibit cellular spreading **(Figure 3.1.1).** Secondly, we utilized a FVD eFluor450, which irreversibly labels dead cells by entering through compromised cell membranes and reacts with amine groups in the cytoplasm (Perfetto et al., 2006). Therefore, FVD eFluor450 resulted in strong fluorescence of dead cells which we then quantified by flow cytometry. Although some binding to surface amine groups occurs in staining live cells, it contributes significantly less to fluorescence and by gating appropriately for background fluorescence using single colour controls, the impact on analysis is negligible (Perfetto et al., 2006). We demonstrated FVD eFluor450 staining of dissociated cells at day 10 in culture showed a mean percentage of viable cells in the slices to be nearly 80% (Figure. 3.1.1). This is similar to Merz et al. and Humpel et al., who demonstrated viability by propidium iodide staining of fixed slices from one hour to 4 weeks. Further, Merz et al. (2012) found maintenance of necrotic areas in the slices in culture H&E staining. Given Merz et al. demonstrated maintained necrosis our finding of approximately, 20% cell death aligns with their finding, although we have yet to perform H&E staining on our slices which would be required to confirm that necrosis is a contributing factor to our 20% inviable cell population. However, although we ask our surgical colleague to obtain tissue at the tumour periphery to minimize explant of regions of necrosis, invariably, some of our samples would contain micro-necrosis. Indeed, it would be interesting for further research and interrogation of this model to 1) analyze the variance of tumour slice's viability away from the average by use of a z-score, and 2) conduct histopathological analysis of our slices to see if our own organotypic slice cultures of GBM recapitulate the results found by Merz et al. (2012) and correspond to the level of cell viability we are seeing by FVD eFluor 450 staining.

We have yet to interrogate our model beyond 10 days, as that is within the experimental timeline. Merz et al. (2013) kept slices viable for up to four weeks, which would be an interesting strategy to pursue in the future. To maintain viability for such long durations, the media could be augmented with supplements such as EGF or FGF as is done with primary GBM cells (Singh et al., 2003), in addition to the growth factors already present in the B27 supplement. However, including serum in the media is to be avoided as it results in differentiation of primary GBM cells (Joseph et al., 2015).

Due to the nature of harvesting the GBM slices, it is likely that some contamination would occur. Throughout the project, sporadic contaminations of what appeared to be yeast were present on the semi-permeable membranes. To address the sterility, all possible components of the vibratome were autoclaved, along with the forceps used for plating and harvesting. Unfortunately, the vibratome is not in a sterile biosafety cabinet, which would further reduce the likelihood of contamination. Although practically challenging, slicing the tissue in a sterile environment would also further reduce the probability of contamination. Utilizing an antibiotic PSQ that is supplemented with anti-mycotic drugs would also be a simple way to further reduce the likelihood of contamination of the culture.

The wide variability in the slices poses some challenges for analysis. It can vary what region of the tumour the slice is taken from, and how much agitation that region received during resection. For example, ultrasonic aspiration is a commonly used neurosurgical technique to remove the bulk of the lesion. If the region of the tumour being prepared for tissue sampling has been exposed to excessive amounts of ultrasonic aspiration, the likelihood of that sample being destroyed is increased, ultimately resulting in reduced viability in culture. It also depends on the consistency of the tumour sample given, as different regions of the tumour have different

textures. For instance, peripheral tumour of the cortex can be very firm with actively proliferating cells, but the internal necrotic core of the tumour is very gelatinous and challenging to slice and culture, to the extent that some samples were unable to be sliced due to their texture and lack of structure. Good communication with the neurosurgeon is key to achieving a successful organotypic culture. We have found that samples from the edge of the tumour, away from the necrotic core that has not been too disturbed by surgical coagulation of aspiration is key to providing tumour slices that are easiest to establish in culture. That is, that they are able to be sliced at a consistent thickness.

Running parallel to slice viability is the proliferative and mitotic activity of the slices. To properly recapitulate the tumour's behaviour *in situ* , it is key that there are regions of proliferating cells to accompany the regions of necrosis. To determine whether or not the cells are proliferating, Merz et al. (2012) utilized a Ki67 assay for immunohistochemical analysis of proliferation. To further validate our model's ability to represent GBM, future research should employ this assay in a subset of slices. Moreover, further research could employ the method utilized by Goliwas et al. (2016) to compare cell density at the beginning and end of the culture period. This method completes fixation, sectioning and staining with hematoxylin and eosin for further histological analysis of cell density (Goliwas et al., 2016). Although this group analyzed cell density in a breast cancer 3D culture, the same method could easily be used on the organotypic slice culture model used here.

A criticism of organotypic slice cultures is significant inter-experimental variability given different tumours and patient samples. However, this is both a benefit and a downside of the model. On one hand, this extreme variability presents a challenge to generate reproducible, robust data that is consistent across patients due to the vast heterogeneity that makes GBM so

challenging to treat. On the other hand, if statistically significant results are achieved, the significant variability is also a benefit of the model, as it increases the likelihood results generated using this model will translate well to the patient population where heterogeneity is the reality. To achieve this, future studies will have to ensure significant sample size is used to provide the appropriate level of certainty. This will require statistical power calculations to determine the number of samples needed (Whitley and Ball, 2002), especially when focusing on clinically translational results.

4.2 Lentiviral Transduction of Organotypic Slice Culture Model of GBM

The novelty of our work is the genetic manipulation of organotypic GBM slices with lentivirus. Previous work by Parker et al., demonstrated slice transduction by using a general retrovirus at a viral titer of 4 CFU/mL. The disadvantage of this virus is that it only infects dividing cells (Howe et al., 2012). We elected to use a lentiviral system as it infects a wider variety of cell types and states and utilized a far-red fluorescent transgene due to reduced autofluorescence in brain slices at the wavelength (Jun et al., 2017). Based on a review of the literature, the autofluorescence is likely coming from a variety of different molecules within the cellular and extracellular environment of the tumour, such collagen, riboflavin, retinol, folic acid NADPH, and tyrosine. (Georgakoudi et al., 2002). The high level of autofluorescence in GBM tissue is primarily due to increased proportions of aforementioned autofluorescent molecules. For instance, GBM's increased energy demand requires higher levels of NADPH (Wahl et al., 2017), which results in higher autofluorescence than present in healthy tissue with normal levels of NADPH. (Georgakoudi et al., 2002; Monici et al., 2005; Guntuka et al., 2016). As proof in principle, we chose to transduce our slices utilizing a far-red expressing lentiviral vector. Our results demonstrated effective far-red lentivirus transduction throughout the thickness of the slice

by confocal microscopy **(Figure 3.3.1).** Subsequent dissociation and flow cytometry analysis showed nearly 20% of the slice expressed far-red fluorescent virus as compared to only roughly 4% in empty vector controls. To achieve this level of transduction, concentration and resuspension of lentivirus was required. This was done to increase viral titre and to minimize the volume of DMEM and serum (the media in which lentivirus is made) added to the culture slices which we demonstrated reduced the viability of slices (Figure 3.3.1). However, depending on the experimental inquiry, improved transduction efficiency may be required. Optimization of transduction conditions to increase the penetration and transduction of the slices will be required going forward. We were able to transduce nearly 20% of the alive cells using 300 μL 10X concentrated virus, which was well over background autofluorescence levels in NV control (5%) and empty vector controls (4%). An option to increase transduction efficiency is to further increase our viral titre delivered to the slices. However, increasing amounts of virus may not necessarily result in increasing levels of far-red fluorescence. As expected, we demonstrated decreased slice viability after lentiviral transduction, therefore it is possible that the highly transduced GBM cells were subsequently gated out during flow analysis. Therefore, a titration curve will need to be performed going forward to determine optimal transduction while maintaining cellular viability.

GBM's invasive nature is key to its recurrence, as it makes complete resection virtually impossible and recurrence inevitable (Lim et al., 2007; Beadle et al., 2008). It has been found that when comparing 2D and 3D *in vitro* invasion assays and 3D rodent slice culture models, there are disparate cellular migration programs (Farin et al., 2006; Beadle et al., 2008; Panopoulos et al., 2011). Notably, this could be a reason for the lack of translation between laboratory results and clinical application. Parker et al. (2017) attempted to address this using a

retroviral vector to visual tumour cell migration *in vitro*. Similar to Merz et al. (2012), they found retention of histological features after 15 days of culture. Parker et al. (2017) were able to utilize these organotypic cultures in several ways. After harvesting intraoperative GBM samples, Parker et al. (2017) infected the organotypic slice and observed cellular migration patterns using live cell imaging This study shows similar results to ours, indicating that organotypic slice cultures are able to be infected by retroviruses and express fluorescence transgenes. Notably, Parker et al. (2017) used a standard retrovirus system, which only infects actively mitotic cells, whereas we used a lentivirus vector with the ability to infect a wide array of both dividing non-dividing cells. Parker et al. (2017) claims that enriching fluorescence within the rapidly growing GBM cell populations can give more clear insight into GBM cell migration without excess labelling of other cell types. However, organotypic GBM slice cultures presumably contain a variety of cells. Our flow cytometry data suggests GFAP+ cells account for 60-70% of cells within the slice, with the remainder of the cells in the slice TME likely being endothelial cells, microglia, neurons, immune cells, and oligodendrocytes. To specifically determine the identity of these cells, staining for other markers could yield a clear picture. Further investigations could search for endothelial cells (CD34), microglia (IBA-1), tumour associated macrophages (TAMS) (CD163), and neurons (Thy-1) (Debinski et al., 2014; Mei et al., 2017; Kvisten et al., 2019). Notably, GFAP is a marker of differentiation in glial cells and therefor it would not stain undifferentiated GSCs (Mei et al., 2017), which possibly accounts for the approximately 3% drop in signal when looking at iRFP-transduced and GFAP double positive cells.

To further study the population in which our lentivirus was infecting, we used a GFAP marker while assaying the slices for iRFP expression by flow cytometry **(Figure 3.3.4)**. We found that the majority of cells expressing iRFP (far-red fluorescence) were also positive for

GFAP, indicating they are of astrocyte lineage and are likely GBM cells (Sereika et al., 2018). Staining for the GSC marker CD133 in dissociated GBM organotypic slice culture samples would be interesting to elucidate the presence of GSCs in the model, and whether our lentiviral system is transducing them. It is tempting to hypothesize that they would be at a low prevalence in the slices, for two reasons. Firstly, GSCs are already at a low percentage of tumour bulk (Lathia et al., 2015; Safa et al., 2015). Secondly, the samples are typically taken from the peripheral edge of the tumour at the site of active proliferation, but GSCs are hypothesized to be present most in the hypoxic core of GBM (Hiddleston et al., 2009).

4.3 Isolation of EVs from organotypic slice culture of GBM

EVs have been shown to have an important role in the GBM TME and this slice culture model has indicated the ability to isolate extracellular vesicles shed into the media. Previous studies have also indicated EVs presence in culture although they have only been found in monocultures of GBM cell lines. Skog et al. (2008) isolated patient-derived primary GBM cells lines, and isolated EVs shed into the media via ultracentrifugation. Interestingly, they found abundant levels of EVs shed into the media that had mRNA signature closely related to the parent cells. These EVs were fluorescently tagged and then cultured with human brain microvascular endothelial cells (HBMVECs), where they were found to be internalized into the brain endothelial cells. These EVs were also shown to stimulate proliferation in HBMV and human U87, further suggesting a strong pro-tumour role in the GBM TME. Our results from this study run parallel to this but are the first to find EVs present in conditioned culture medium from our organotypic GBM slices, which were positive for EV marker CD63 and CNS tumour marker GD2 **(Figure 4.3.1)**. However, GD2 is not an ideal GBM marker, and further studies will introduce GBM specific markers such as EGFRvIII (if present in the molecular landscape of

parent tumour) or GFAP. Our collaborators at the ACRI have attempted to initially probe for GFAP and CD133 on the surface of EVs from CCM, but it has proven to be challenging. It is hypothesized that media components are resulting in non-specific binding prior to nanoflow cytometry analysis, and more work is necessary to determine the feasibility of staining for such markers in this EV population. Moreover, given the presence of only one female patient in samples analyzed for EVs from CCM, further studies should incorporate a more sex-balanced sample size to account for sex differences between male and female patients.

EVs have also been shown to have significant potential in liquid biopsy in GBM and other cancers (Osti et al., 2018; Chi et al., 2020). Osti et al. (2018) found that EVs were detectable in patient plasma at higher levels than healthy controls, and that those circulating EVs have a GBM-specific proteomic signature. These GBM-specific EVs in patient circulation have been found to represent up to 10% of all EVs in patient plasma and these EVs have just as extensive heterogeneity as the parent tumour in which they are derived (Fraser et al., 2018). With respect to EV-based tracking of treatment response, Chi et al. (2020) found a pre-treatment EV transcriptome signature that could distinguish between patients who had durable benefit versus those with rapid progression of post-treatment disease. This study also found a unique EV sRNA signature between GBM patients and healthy controls (Supplemental Figure 3.) in preoperative plasma samples. Future analysis will aim to analyze EV-sRNA in CCM for unique signature, or matching signature as this has not yet been conducted.

4.4. Future Directions and Concluding Remarks

We have shown that this organotypic slice culture model of GBM stays viable in culture for 10 days. Moreover, we have found that the representative model is amenable to lentiviral genetic manipulation which was demonstrated by the insertion of a far-red fluorescent protein.

This expression was demonstrated throughout the slice, which indicates that the virus was able to penetrate successfully. This was also quantified using flow cytometry, which showed an average transduction of nearly 20%. Finally, we found extracellular vesicles to be shed into the media of the organotypic slices, adding more utility to the model of GBM.

Further tweaking of the viral load given is required for optimal transduction of the slices. Although a significant amount of virus did result in measurable fluorescence, adding more virus may contribute to increased cell death within the slices. . Therefore, the cells that are expressing iRFP may be dying and lowering our effective transduction efficiency. This may be due to the increased number of viral particles resulting in potential integration events, increasing the likelihood of integration occurring in the location of the target cell's DNA which becomes catastrophic. To achieve optimal virus concentration, further studies will titrate different amounts of virus onto the slices to find the most amount of fluorescence achievable while keeping viability within acceptable parameters.

Further studies utilizing this model system can work towards answering numerous questions. Parker et al. (2017) analyzed VEGF secretion from the cells in response to hypoxia. Previous work in our lab has utilized a hypoxia assay to study how GBM cell cultures adapt to stress (Attwood et al., 2020) and would be a great candidate for future use of this model. Organotypic slice cultures can be transduced using iRFP-expressing lentivirus prior to exposure to hypoxia. Following hypoxia, the far-red fluorescent expressed by cells within the slice could be tracked and analyzed for migration in response to diminished oxygen supply. Hypoxia is not the only stressor that could be applied to the slices to analyze how they react to environmental stressors. iRFP-expressing lentivirus infected GBM organotypic slice cultures can be given chemotherapy and irradiated as done by Merz et al. (2012). These slices could then be analyzed

for migration of far-red fluorescent cells or stained for CD133 to see if there is an enrichment in GSCs following standard of care treatment for GBM. Previous work in our lab has also generated CRISPR/Cas9 guide RNA sequences compatible with our second-generation lentiviral system. It is tempting to speculate that the successful lentivirus-mediated iRFP insertion achieved in this project has the potential application of inserting CRISPR/Cas9 sequences into the DNA of our slices. This is an exciting stream of research that may yield more answers about GBM genetics in the TME. For instance, migration and invasion could be studied by knock-down of genes associated with migration and invasion, and then track movement throughout the slice.

The preliminary isolation of extracellular vesicles from the media of the organotypic GBM slice cultures has multiple avenues of future research. Importantly, preliminary data suggest that these EVs are positive for canonical EV markers as outlined in MISEV (2018) as the field standard. More specific GBM markers are to be used (GFAP, CD133) to further validate that these EVs are indeed GBM-derived. Another way to do this is not to look for EV surface molecules and markers but to investigate EV cargo. Initial data from our collaboration with the ACRI indicates there may be a GBM-specific signature in sRNA profiles within EVs from patient plasma samples. Further work can be done to determine whether or not this sRNA signature is also present in CCM-isolated EVs. With this, organotypic slice cultures can be manipulated in a variety of ways. For instance, Chi et al. (2020) found that EV transcriptome signature is able to distinguish GBM patients who had durable benefit to the chemotherapeutic dacomitinib versus those patients who experienced rapid progression (Chi et al., 2020). This same methodology could be applied by treating slices with chemotherapy and determining whether CCM-derived EV also can predict *in-vitro* treatment response. The same concept applies

to lower grade tumours as well, for if the EV signature changes between the culture of low grade and high-grade astrocytoma, it could lend valuable insights into potential liquid biopsy targets, indicating when transformation to high grade malignancies occur. Specifically, if distinct EV cargo is present between the culture of low-grade tumours and high-grade tumours, this signature may be clinically detectable by taking longitudinal blood samples of low-grade tumours. The model could then be used to screen that patient's potential response to therapy. Although exciting that this type of precision, targeted screening in the organotypic slice culture model may be possible, further research is needed in order to achieve these outcomes. We were able to show far-red fluorescence in the organotypic GBM slices, and this far-red fluorescence may be packaged and expressed in EVs as well. If these EVs are active in paracrine signalling as shown previously (Skog et al., 2008; Wang et al., 2019; Hallal et al., 2002), far-red fluorescent labelling could illuminate where the EV migration and the role they play in cellular communication. If far-red fluorescent EVs isolated from GBM CCM were to be given back to a naive slice from same tumour, it would be interesting to see if those EVs are able to be taken up into the naive slice, and how the EVs shed by the naive tumour change. This schema of experiment could also be done incorporating environmental stressors such as hypoxia, chemotherapy, or radiation to see how the message changes. Perhaps, the increase in pro-angiogenic factors secreted and transported by GBM EVs found in Wang et al. (2019) would be even more upregulated in the naïve slice if the parental tumour slice were exposed to a hypoxic environment.

In summary, we have developed an organotypic slice culture model of GBM, that is representative of the genetics of GBM, while preserving the 3D TME of the highly heterogeneous malignancy. The model is able to stay viable in culture conditions, and is amenable to genetic manipulation, evidenced by the lentivirus-mediated insertion of a far-red

fluorescent protein. This far-red fluorescence was observed throughout the thickness of the slice and achieved a nearly 20% transduction of the cells as a whole. This study also was able identify extracellular vesicle-sized particles from the media of organotypic GBM slices, which were positive for canonical EV markers and therefor are suspected to indeed be EVs. Further work to be done on the former front will utilize the lentiviral delivery system to study GBM *in vitro.* Further work on the latter front will integrate the lentiviral manipulation of the slices, analysis of EVs into the CCM of the slices, and attempt to connect the EVs found in culture to those found in matched patient blood samples. Taken together, this study has established and utilized a powerful model for studying GBM.

REFERENCES

Ackerman, D., et al. Hypoxia, lipids, and cancer: surviving the harsh tumor microenvironment. *Trends in Cell Biology* **8,** 472-478 (2014).

Anderson, P., et al. stress granules: the tao of RNA triage. *Trends in Biochemical Sciences* **3,** 141-150 (2008).

Agnihotri, S., et al. A GATA4-regulated tumor suppressor network represses formation of malignant human astrocytoma. *Journal of Experimental Medicine* **208**, 689-702 (2011)

Alves, T.R. et al. Glioblastoma cells: A heterogeneous and fatal tumor interacting with the parenchyma. *Life Sciences* **89**, 532-539 (2011).

Anido, J. et al. TGF-beta receptor inhibitors target the CD44(high)/Id1(high) glioma initiating cell population inhuman glioblastoma. *Cancer Cell* **18**, 655-688 (2010)

Arimoto, K., et al. Formation of stress granules inhibits apoptosis by suppressing stress-responsive MAPK pathways. *Nature Cell Biology* **11,** 1324-1332 (2008)

Bailey, P., Cushing, H. A classification of the tumors of the glioma group on a hestogenetic basis with. A correlated study of prognosis. Philidelphia: J.B. Lippincott Company. 1926.

Banerjee S., et al. Neurofromatosis-1 regulates mTOR-mediates astrocyte growth and glioma formation in TSC/Rheb-independent manner. *Proceedings of the National Academy of Science US* **108,** 15996-6001 (2011).

Bayin, N.S., et al. Patient specific screening using high-grade glioma explants to determine potential radio-sensitization by TGF-beta small molecule inhibitor. *Neoplasia* **18,** 795-805 (2016).

Bs, C., et al. Expert opinion of investigational drugs glioblastoma multiforme: a review of where we have been and where we are going. 3784 (2016).

Campos, B., et al. Expression of nuclear receptor corepressors and class 1 histone deacetylases in astrocytic gliomas. *Cancer Science* **102,** 387-292 (2011)

Chen, R., et al. A hierarchy of self-renewing tumor-initiating cell types in glioblastoma. *Cancer Cell* **17**, 362-375 (2010)

Cheng, W. et al. Bioinformatic profiling identifies an immune-related risk signature for glioblastoma. *Neurology* **24,** 2226- 2234 (2016).

CBTRUS. Primary brain and central nervous system tumors diagnosed in the United States in 2004-2008. http://www.cbtrus.org/2012-NPCR-SEER/CBTRUS_Report_2004-2008_8-23-2012pdf;2012.

Davis, M.E. Glioblastoma: overview of disease and treatment. *Journal of Oncology Nursing* **5,** 1-8 (2016).

DeAngelis, L.M. Brain tumors. *The New England Journal of Medicine* **344**, 114-23 (2001).

Dione, K.R., Tyler, K.L. Neuronal Cell Culture, 1078, 97-117. (2013)

Ekstand, A.J., et al. amplified and rearranged epidermal growth factor receptor genes in human glioblastoma reveal deletions of sequences encoding portions of the N- and/or C-terminal tails. *Proceedings of the National Academy of Sciences USA* **89,** 4309-4313.

Esteller, M. Cancer epigenomics: DNA methylomes and histone-modifications maps. *Nature Reviews Genetics* **8,** 286-298 (2007).

Fraser , K., et al. Characterization of single microvesicles in plasma from glioblastoma patients. *Neuro-Oncology* **21**, 606-615 (2018).

Furnari, F.B., et al. malignant astrocytic glioma: genetics, biology, and paths to treatment. *Genes and Development* **21,** 2683-2710 (2007).

Goliwas, K.F., Miller, L.M., Marshall, L.E., Berry, J.L.,

Gould, C.M., Courtneidge, S.A. Regulation of invadopodia by the tumor microenvironment. *Cell Adhesion and Migration* **3**, 226-235 (2014).

Hardee, M.E. et al. Resistance of glioblastoma-initiating cells to radiation mediated by tumor microenvironment can be abolished by inhibiting transforming growth factor beta. *Cancer Res.* **72**, 4119-4129 (2012).

Hegi, M.E., et al. MGMT gene silencing benefit from temozolomide in glioblastoma. *The New England Journal of Medicine.* **352**, 997-1003 (2005).

Humpel, C. Neuroscience forefront review organotypic brain slice cultures: A review. *Neuroscience* **305**, 86-96 (2015).

Huse, J.T., Holland, E.C. Targeting brain cancer: advances in molecular pathology of malignant glioma and medulloblastoma. *Nature Reviews Cancer* **5**, 319-331 (2010)**.**

Inda, M.M., et al. Tumor heterogeneity is an active process maintained by a mutant EGFR-induced cytokine circuit in glioblastoma. *Genes and Development* **24,** 1731-1745 (2010).

Jamal, M. et al. The brain microenvironment preferentially enhances the radioresistence of CD133(+) glioblastoma stem-like cells. *Neoplasia* **2**, 150-158 (2012)

Kastenhuber, E.R., Lowe, S.W. Putting p53 in context. *Cell* **170,** 1062-1078 (2017).

Kedersha, N., et al. Stress granules and cell signaling: more than just a. passing phase? *Trends in Biochemical Sciences* **10,** 494-506 (2013).

Kim, T.Y., et al. Epigenomic profiling reveals novel and frequent targets of aberrant DNA methylation-mediating silencing of malignant glioma. *Cancer Research* **66**, 7490-7501 (2006)

Knudson, A.G. Mutation and cancer: statistical study of retinoblastoma. *Proceedings of the National Academy of Sciences USA* **4**, 820-823 (1971)

Louis, D.N. et al. The 2007 WHO classification of tumors of the central nervous system. *Acta Neuropathologica* **114**, 97-109 (2007).

Marques-Torrejon, M.A., et al. Modelling GBM tumor-host. Cell interactions using adult brain. Organotypic slice co-culture. *disease Models and Mechanisms* **11** (2018).

Merz, F., et al. Organotypic slice cultures of human GBM reveal different susceptibilities to treatments. *Neuro-Oncology* **6,** 670-681 (2013).

Ohgaki, H., Kleihues, P. Epidemiology and etiology of gliomas. *Acta Pathologica* **109**, 93-108 (2005).

Palmieri, D. et al. The biology of metastases is a sanctuary site,. *Clin Cancer Research* **13,** 1656-1662

Parker, J.J., et al. A. human glioblastoma organotypic slice culture model for study of tumor cell migration and patient-specific effects of anti-invasive drugs. *Journal of Visualized Experiments* **125** (2017)

Parsons, D.W., et al. An integrated genomic analysis of human glioblastoma multiforme. *Science* **321,** 1907-1812 (2008)

Phillips, H.S., et al. Molecular subclasses of high-grade glioma predict prognosis, delineate a pattern of disease prognosis and resemble stages in neurogenesis. *Cancer Cell* **9,** 157-173 (2006)

Shamir, E.R., Ewald, A.J. Three-dimensional organotypic culture: experimental models of mammalian biology and disease. *Nature Review Molecular Cell Biology.*

Singh, S.K., et al. Identification of a cancer stem cell in human brain tumors. *Cancer Research* **63,** 5821-5828 (2003)

Singh, S.K., et al. identification of human brain tumour initiating cells. *Nature* **432:** 396-401 (2004)

Stupp, R., et al. Effects of radiotherapy with concomitant and adjuvant temozolomide versus radiotherapy alone on survival in glioblastoma randomized phase III study: 5 year analysis of the EORTC-NCIC trial. *Lancet Oncology* **10,** 459-466 (2009).

Torsvik, A. et al. U-251 revisited: genetic drift and phenotypic consequences of long-term cultures of glioblastoma cells. *Cancer Medicine* **4**, 812-824 (2014).

TCGA CGARN. Comprehensive genomic characterization defines human glioblastoma genes and core pathways. *Nature* **455,** 1061-1068 (2008).

Verhaak, R.G., et al. Integrated genomic analysis identifies clinically relevant subtypes of glioblastoma characterized by abnormalities in PDGFRA, IDH1, EGFR, and NF1. *Cancer Cell* **17,** 98-110 (2010).

Vilas-Boas, F. et al. Impairment of stress granule assembly via inhibition of the e1F2alpha phosphorylation sensitized glioma cells to chemotherapeutic agents. *Journal of Neuro-oncology* **2**, 253-260 (2016).

Wang, M., et al. Role of tumor microenvironment in tumorigenesis. *Journal of Cancer* **5,** 761-773 (2017).

Wen, P.Y., et al. Malignant gliomas: strategies to increase the effectiveness of targeted molecular treatment. *Expert Review of Anticancer Therapy* ***6,*** 733-754 (2006).

APPENDIX A SUPPLEMENTARY DATA

Figure A.1. Ependymoma organotypic slice culture show reduced viability in culture. Ependymoma slices were culture for 10 days, dissociated and stained for eFluor450 and analyzed for flow cytometry to determine percent viability. **(A)** Ependymoma slices were dissociated, stained for FVD eFluor450 and prepared for analysis by flow cytometry at day 2, 6 and 10 in culture. Cellular debris was excluded based on forward and side scatter (far left panel). Doublet discrimination was then carried out based on side scatter-width and side scatter-height (center panel). Cell viability was analyzed by setting FVD eFluor450 negative gate based on heat shocked controls and universal negative. **(B)** Quantification of percentage of cells viable by FVD eFluor450. n=1 slice for each time point.

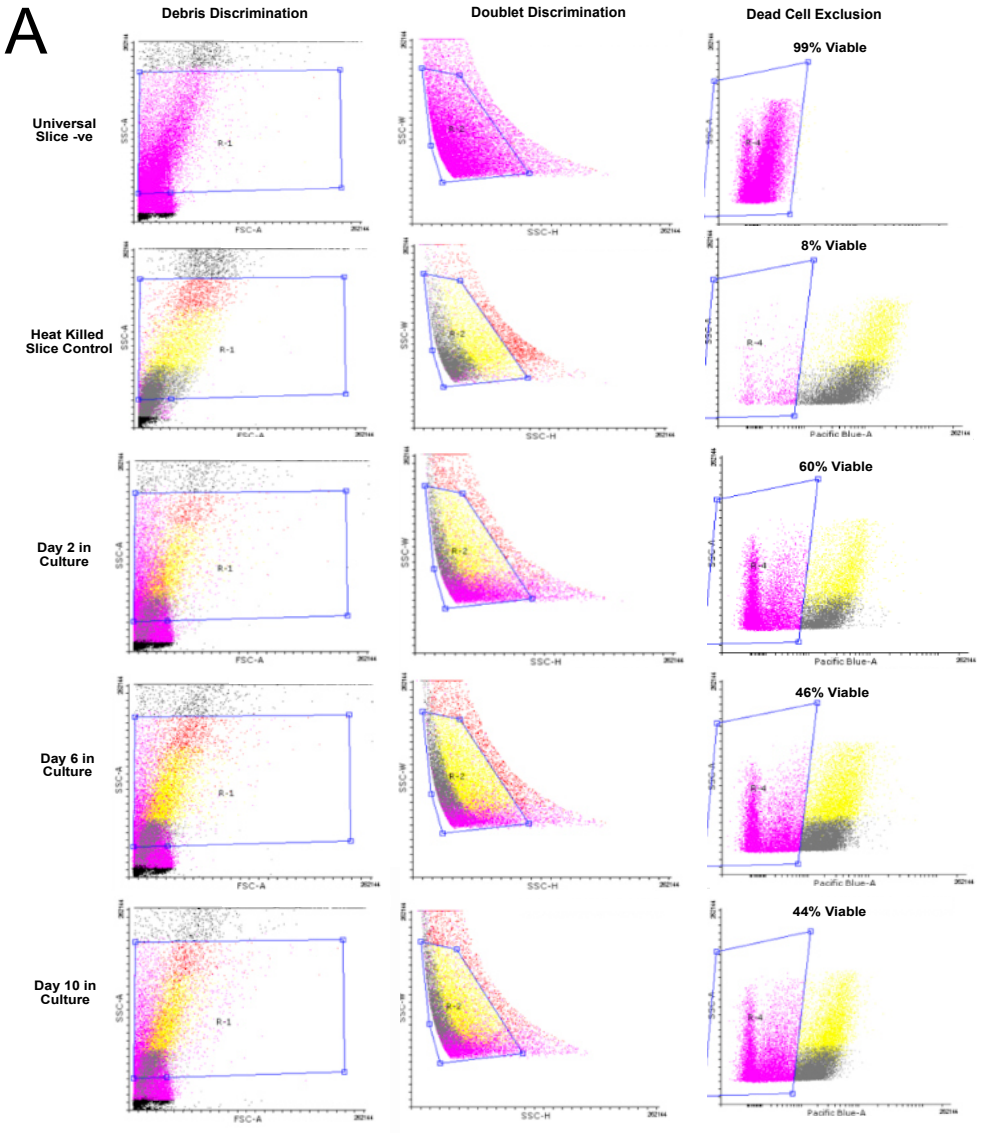
A
Debris Discrimination
Doublet Discrimination
Dead Cell Exclusion
Universal Slice -ve
99% Viable
Heat Killed Slice Control
8% Viable
Day 2 in Culture
60% Viable
Day 6 in Culture
46% Viable
Day 10 in Culture
44% Viable
B
% CELLS VIABLE
0
10
20
30
40
50
60
70
Day 2
Day 6
Day 10
DAYS IN CULTURE

Figure A.2. GBM patient plasma derived Vn96-captured EV sRNA cluster together. Preoperative blood samples were taken from arterial line prior to craniotomy and processed for Vn-96 captured EV analysis. Unsupervised hierarchal clustering heat-map of sRNA sequencing of plasma Vn96-EV sRNA between astrocytoma (n=4; GBM 1,3,4,5) and healthy controls, (ACRI069, prostate018, prostate022, ACRI022, ACRI022, ARCI075). Data shown are regions with false discovery rate of <0.05. Analysis conducted by ACRI.

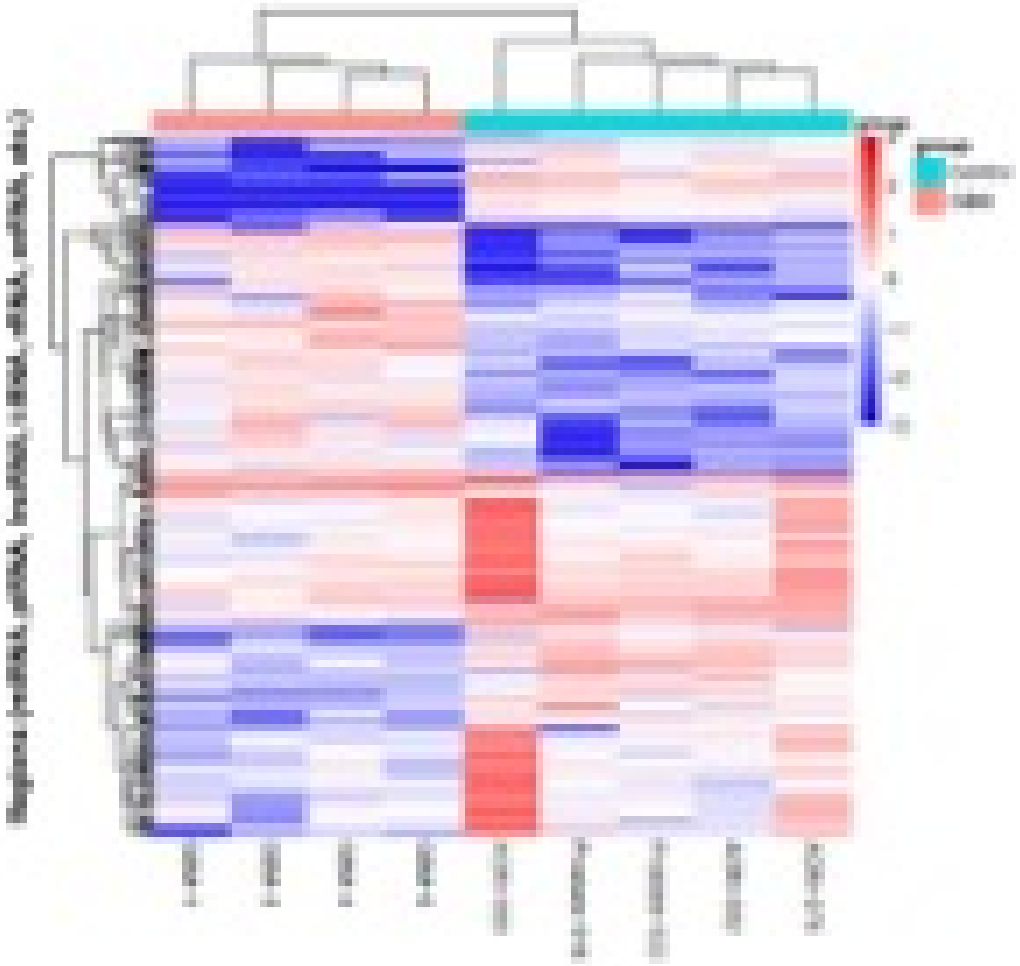

Figure A.3. Gating strategy in entirety for lentiviral functional titration. U-251 MG glioma cells were transduced with concentrated iRFP expressing lentivirus resuspended in DMEM or neurobasal at varying dilutions. Percentage of total iRFP+ cells were used to calculate physical titration of lentivirus. Representative flow cytometry gating strategy and analysis of debris discrimination, viable cell inclusion, iRFP+ cell inclusion, and iRFP+ cells of viable cells.

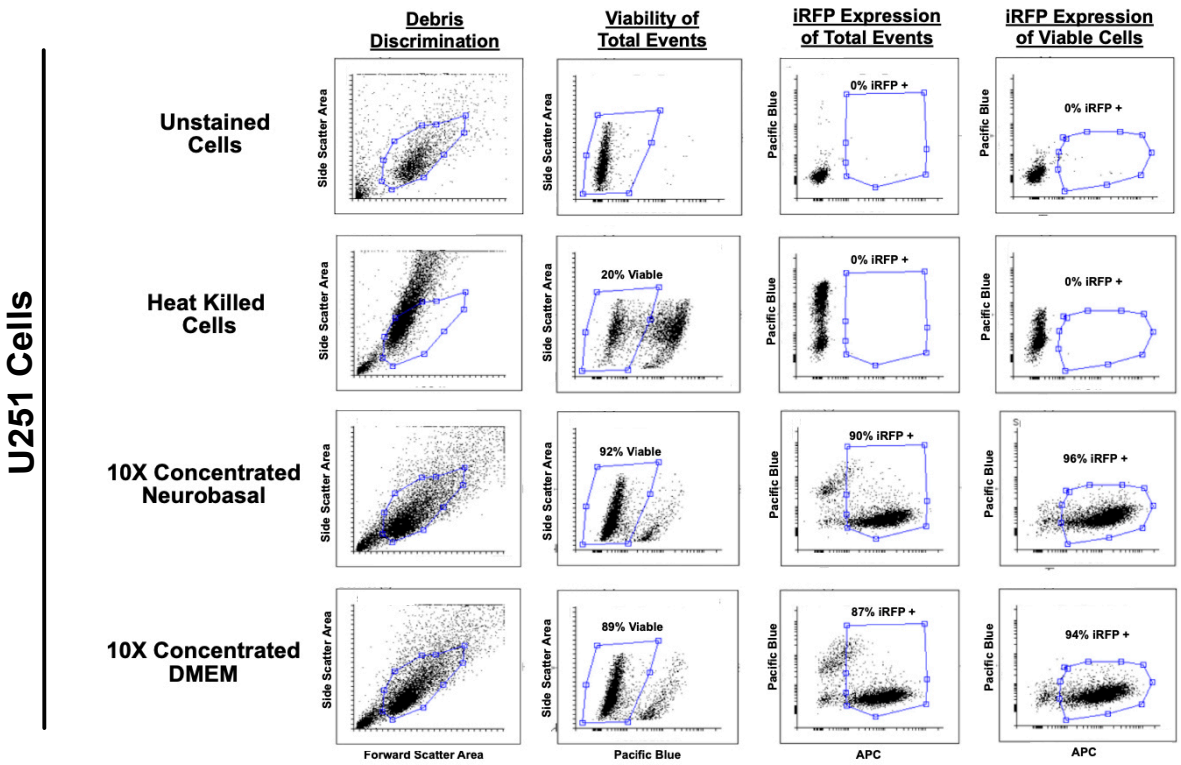
U251 Cells
Debris Discrimination
Viability of Total Events
iRFP Expression of Total Events
iRFP Expression of Viable Cells
Unstained Cells
Heat Killed Cells
10X Concentrated Neurobasal
10X Concentrated DMEM
Side Scatter Area
Forward Scatter Area
Pacific Blue
APC
0% iRFP +
20% Viable
90% iRFP +
92% Viable
96% iRFP +
87% iRFP +
89% Viable
94% iRFP +

Supplemental Table 1. Patient/sample information for extracellular vesicle analysis.

Sample	Age	Sex	Gender	Tumour Type
AW001	36	Male	Male	GBM
AW002	57	Male	Male	GBM
AW004	70	Female	Female	GBM
AW005	58	Male	Male	GBM
AW006	41	Male	Male	GBM
AW007	42	Male	Male	GBM